revision 1

Crystal chemistry of layered Pb oxychloride minerals with PbO-related structures. I. Crystal structure of hereroite, $[Pb_{32}O_{20}(O,\square)](AsO_4)_2((Si,As,V,Mo)O_4)_2Cl_{10}$

Oleg I. Siidra[1], Sergey V. Krivovichev[1], Rick W. Turner[2], Mike S. Rumsey[3], John Spratt[3],

[1] Department of Crystallography, St. Petersburg State University, 7–9 University Emb., St. Petersburg 199034, Russia;

[2]The Drey, Allington Track, Allington, Salisbury SP4 0DD, Wiltshire, UK;

[3]Mineralogy Department, Natural History Museum, Cromwell Road, London, SW7 5BD, UK.

* Corresponding author. E-mail: siidra@mail.ru

Abstract

The crystal structure of hereroite, a new complex lead oxychloride mineral from the Kombat Mine, Grootfontein, Namibia, has been solved by direct methods and refined to $R_1 = 0.054$ for 6931 unique observed reflections. The mineral is monoclinic $C2/c$, $a = 23.139(4)$, $b = 22.684(4)$, $c = 12.389(2)$ Å, $\beta = 102.090(3)^o$, $V = 6358.8(18)$ Å^3. The structure contains 16 independent Pb sites in strongly asymmetric coordination by O and Cl atoms. There are two tetrahedral sites, from which one (As) is occupied solely by As, whereas the second (T) has the mixed occupancy of $[Si_{0.48}As_{0.29}V_{0.15}Mo_{0.09}]$. There are in total 21 O sites. The O1-O8 sites belong to the AsO_4 and TO_4 tetrahedral oxyanions. The other O atoms (O9-O20) are tetrahedrally coordinated by Pb atoms, thus being central for the OPb_4 oxocentered tetrahedra. The OPb_4 tetrahedra share edges to form the $[O_{21}Pb_{32}]^{22+}$ layers that can be described as derivatives of the [OPb] layer from the structure of tetragonal PbO (litharge). The $[O_{21}Pb_{32}]^{22+}$ layer in hereroite can be obtained from the [OPb] layer by

removal of blocks of oxocentered tetrahedra, which results in formation of double-square sevenfold and square fourfold cavities. The cavities are occupied by the AsO_4 and TO_4 tetrahedra, respectively. The topology of the $[O_{21}Pb_{32}]^{22+}$ layer is rather complex and can be described as a combination of modules extracted from the layers of OPb_4 tetrahedra present in the structures of kombatite and symesite. The topological functions of tetrahedra within the layer are analysed using the square lattice method, which shows that each symmetry-independent tetrahedron has its own topological function in the layer construction. The structure of hereroite belongs to the 2:1 type of layered Pb oxyhalides and consists of alternating PbO-type layers and Cl sheets oriented parallel to the (010) plane.

Keywords: hereroite; lead oxyhalides; crystal structure; litharge derivatives; layered structures, oxocentered tetrahedra, modular structures, method of square lattices.

Introduction

Lead oxyhalides occur under a wide range of natural and technological conditions (Post and Buseck, 1985; Welch et al. 1996, 1998, 2000, 2001; Noren et al. 2002; Turner, 2006; Cziczo et al. 2009; Kampf et al. 2010a, b; Turner and Rumsey, 2010). Their formation and precipitation play an important role in the transport of Pb from mines and mill tailings to the biosphere. Lead oxyhalides are also important as inorganic materials with various existing and potential technological applications (Matsumoto et al. 2001; Sigman and Korgel, 2005; Pfitzner and Pohla, 2009; Wan et al. 2011). In nature, lead oxychlorides occur as secondary minerals in oxidation zones of mineral deposits. Their structures may accommodate a wide range of elements, including As, S, V, Mo, P, Si, I, *etc*., which results in interesting chemical and structural diversity. Of particular interest are minerals with layered PbO-derivative structures, which are structurally related to the Aurivillius phases. Table 1 provides details on chemical composition and crystallographic data for natural PbO-related oxychloride minerals known to date. In this paper, we report on the crystal structure of hereroite, $[Pb_{32}O_{21-x+y}](AsO_4)_2((Si_x(As,V)_{1-x-y}Mo_y)O_4)_2Cl_{10}$, a new complex lead oxychloride mineral recently described from the Kombat Mine, Grootfontein, Namibia (Turner et al. 2012a). Hereroite was found in close association with asisite, damaraite, kombatite, sahlinite, vladkrivovichevite, barysilite, quartz, native copper, hausmannite, jacobsite and manganite. The Kombat mine ore bodies contain primary Pb-Cu-Zn (-Ag) sulfides, which were originally emplaced hydrothermally as fracture fillings. Primary ores were then modified by later epigenetic, hydrothermal and metasomatic replacement events. These events created a range of Pb-Mn-Fe silicate minerals in the Kombat deposit, as well as a variety of late-stage Pb-oxychloride minerals including hereroite (Cairncross, 1997). Hereroite occurs as transparent to translucent intergrown, glassy-looking orange grains up to ~0.5 mm in diameter.

Background information

The crystal structures of PbO-related layered lead oxyhalides are based upon the O-Pb layers alternating with the sheets *X* of X^- ions (X = Cl, Br) (Aurivillius 1982, 1983; Krivovichev et al. 2009). The stacking sequence of sheets is either:

…*X*|OPb|OPb|*X*|OPb|OPb |… with the (OPb):*X* ratio equal to 2:1 (*X* = F, Cl, Br) or

…*X*|OPb|*X*|OPb|*X*… with (OPb):*X* = 1:1.

The 2:1 structure has also been observed in synthetic Aurivillius phases, kombatite, sahlinite, asisite and parkinsonite, whereas the examples of the 1:1 structure are symesite, schwartzembergite, blixite, and mereheadite.

The O-Pb layers can be viewed as derivatives of the [OPb] layer from the structure of litharge, a tetragonal modification of PbO (Boher et al. 1985) (Fig. 1a). The relationships between the structures of litharge and its oxychloride derivatives can be conveniently described in terms of structural units based upon anion-centered tetrahedra. This approach to the description of complex inorganic crystal structures has many advantages over the traditional cation-centered description where the structure contains so-called 'additional' O atoms, coordinated by di- and trivalent cations only [see (Krivovichev and Filatov, 1999a, b; Krivovichev et al. 2004; Siidra et al. 2008c) for reviews and (Chen et al. 2009; Huvé et al. 2009; Mauck et al. 2010; Li et al. 2011; Kampf et al. 2011; Reshak et al. 2012; Endara et al. 2012) for recent applications]. The structure of litharge is usually described in terms of the OPb_4 oxocentered tetrahedra, sharing edges to form [OPb] layers (O'Keeffe and Hyde, 1996). Transformation of the [OPb] layer into one of its derivatives corresponds to the removal of blocks of the OPb_4 tetrahedra from the former (Fig. 1b,c). The resulting layers have the chemical composition $[Pb_mO_n]^{z+}$, with m > n. The role of the *X* sheets is to compensate the positive charge of the O-Pb layers. However, a number of additional modifications has also been observed: (1) substitution of the OPb_4 tetrahedra in the [OPb] layer by tetrahedral or triangular anions such as SO_4 (symesite), MoO_4 (parkinsonite), VO_4 (kombatite), AsO_4 (sahlinite), SiO_4 (asisite), CO_3 and BO_3 (mereheadite) etc.; the substitution may be disordered (as in parkinsonite and asisite) or ordered as in symesite, kombatite and sahlinite; (2) $O^{2-} \leftrightarrow OH^-$ substitution in the [OPb] layers (as observed in blixite and mereheadite); (3) insertion of additional

Pb atoms into the *X* sheet (observed in mereheadite and synthetic $Pb_{31}O_{22}Br_{10}Cl_8$ (Krivovichev et al. 2006)); (4) $O^{2-} \leftrightarrow F^-$ substitution in the [OPb] layers (observed in rumseyite (Turner et al. 2012b)).

Experimental

Chemical composition

According to Turner et al. (2012a), the empirical formula for hereroite based on the assumption of Pb = 32 *apfu* is $[Pb_{32}O_{20.70}]$ $(AsO_4)_2$ $((Si_{0.48}As_{0.29}V_{0.15}Mo_{0.09})O_4)_2Cl_{9.84}$ which gives the simplified formula $[Pb_{32}O_{21-x+y}](AsO_4)_2((Si_x(As,V)_{1-x-y}Mo_y)O_4)_2Cl_{10,}$ where x = 0.48, y = 0.08. The corresponding ideal formula can be written as $[Pb_{32}O_{20}(O,\square)](AsO_4)_2((Si,As,V,Mo)O_4)_2Cl_{10}$.

Single crystal X-ray diffraction study

A transparent equant orange crystal was studied using a Bruker Smart Apex II diffractometer at the Department of Crystallography, St. Petersburg State University, Russia. More than a hemisphere of X-ray diffraction data (θ_{max} = 36.15°) with frame widths of 0.3º in ω, and with 45 s spent counting for each frame was collected at room temperature using the MoKα radiation. The data were integrated and corrected for absorption with an empirical ellipsoidal model using the Bruker programs *APEX* and *XPREP*. The observed systematic absences were consistent with space group *C*2/*c*. The structure was solved by direct methods and refined to R_1 = 0.053 on the basis of F^2 for all unique data. The *SHELX* program package was used for all structural calculations (Sheldrick, 2008). The final model included all atomic positional parameters, anisotropic-displacement parameters for all atoms except oxygen, and a refinable weighting scheme for the structure factors. The final atomic coordinates and displacement parameters are given in Table 3, and selected interatomic distances in Table 4. The list of observed and calculated structure factors can be provided by the authors upon request.

Results

Cation coordination

The structure of hereroite contains 16 symmetrically independent Pb sites. Figure 2 shows the coordination of the Pb atoms with all the bonds shorter than 3.5 Å taken into account. The coordination configurations of the Pb atoms are variable and fall into two groups. Pb1, Pb2, Pb3, Pb5, Pb6, Pb7, Pb11, Pb13, and Pb16 sites are coordinated by the O^{2-} anions in one coordination hemisphere. The number of the O atoms varies from three to four with Pb-O bonds in the range of 2.24-2.96 Å. In the opposite hemisphere, the above mentioned Pb atoms form from three to four long Pb-Cl bonds in range of 3.04-3.48 Å. Pb4, Pb8, Pb9, Pb10, Pb12, Pb14, and Pb15 have strongly asymmetrical coordinations by the O^{2-} anions only. The observed distortion of Pb coordination polyhedra in hereroite is due to the stereoactive behaviour of the $6s^2$ lone electron pairs. Recent study by Walsh et al. (2011) suggests also that distortion in Pb coordination depends on the electronic states of the coordinated anions and is the result of direct electronic interaction between the cation *s* and anion *p* orbitals. Our previous studies of Pb oxyhalides (Krivovichev and Burns 2001a, b, 2002, 2006; Siidra et al. 2007a, b, c; 2008a, b) support this conclusion by demonstration that halide ions and lone pairs on Pb^{2+} cations associate in the same regions of the crystal structures. This phenomenon can be interpreted as a sign of the soft-soft attraction between halide ions and lone electron pairs known as halophilicity of the lone electron pairs.

The structure of hereroite contain two tetrahedrally coordinated sites. The As site is coordinated by four O anions with the <As-O> bond length equal to 1.70 Å. The AsO_4 tetrahedra are disordered with the O8 site split into the O8A (S.O.F. = 0.58(3)) and O8B (S.O.F. = 0.42(3)) sites. The second tetrahedral site, *T*, has mixed occupancy and the <*T*-O> bond length is 1.65 Å. The occupancy of this site can be written as $[Si_{0.48}As_{0.29}V_{0.15}Mo_{0.09}]$, in accordance with the chemical data. Similar mixed-

143 occupied Si sites with the individual *T*-O distances comparable to those in hereroite occur in the
144 structures of dixenite and saneroite (Nagashima and Armbruster, 2010).

145 The total number of oxygen sites is 21. The O1-O8 sites are bonded to As and T sites, being
146 part of strong tetrahedral oxyanions. All other O atoms (O9-O20) are tetrahedrally coordinated by Pb
147 atoms, which results in the formation of oxocentered OPb_4 tetrahedra (Fig. 3). The O9 site is partly
148 occupied and plays the important role for charge-balance compensation between cationic and anionic
149 parts of the structure. The <O-Pb> distances within the OPb_4 tetrahedra are in the range of 2.28-2.35 Å,
150 which is in good agreement with the average value of 2.33 Å derived by Krivovichev et al. (1998).

151 There are five symmetrically independent Cl atoms coordinated by eight Pb atoms each, which
152 is typical for Pb oxyhalides.

153 Bond-valence sums for the cations and anions in the structure of hereroite are listed in Table 2.
154 They are in general agreement with the expected oxidation states, taking into account mixed occupancy
155 for the T site and corresponding deviations of bond-valence sums for the O atoms of the TO_4 tetrahedra
156 (O1, O2, O3, and O4).

157

158 Structure description

159

160 The structure of hereroite (Fig. 3c) belongs to the 2:1 type and consists of alternating PbO-type
161 layers and Cl sheets oriented parallel to the (010) plane. The PbO-type layer is a derivative of the [OPb]
162 tetrahedral layer in litharge and can be obtained from the latter by removal of blocks of oxocentered
163 tetrahedra. The AsO_4 and $(Si,As,V,Mo)O_4$ tetrahedral anions locate in cavities within the PbO-type
164 layer. The formula of the layer can be written as $[O_{20}(O,\square)Pb_{32}]$ taking into account the partly occupied
165 O9 site. The atomic structure of the layer including O9 atoms is shown in Figure 4a. Figure 4b shows
166 the same layer viewed from the standpoint of oxocentered OPb_4 tetrahedra in polyhedral representation.
167 Neglecting the low occupancy of the O9 site, the formula of the layer can be written as $[O_{21}Pb_{32}]^{22+}$
168 (Fig. 4c). There are two types of vacant cavities in the layer: a double-square sevenfold cavity and a

square fourfold cavity. The former is occupied by the AsO_4 tetrahedron, whereas the latter is occupied by the mixed TO_4 tetrahedron. The size of the cavities obviously correlates with the size of the tetrahedral anions: larger arsenate tetrahedra occupy larger cavities, whereas smaller tetrahedra occupy smaller cavities. The difference in size is rather small, but should not be neglected. This conclusion is supported by the observations of the structures of other Pb oxychlorides: the larger $(AsO_4)^{3-}$ and $(VO_4)^{3-}$ anions in kombatite and sahlinite occupy sevenfold cavities, whilst smaller $(SO_4)^{2-}$ anions occupy the fourfold cavities in symesite. As a result, the structure of the $[O_{21}Pb_{32}]^{22+}$ layer in hereroite may be described as a combination of the symesite and kombatite modules (Fig. 1d) organized into alternating diagonal stripes. Figure 4c shows the structure of the Cl sheet in hereroite, which is a vacancy-free square sheet of Cl ions typically observed in Pb oxyhalides.

Discussion

Topological features of the O-Pb tetrahedral layers in lead oxyhalides can be described using the method of square lattices (Krivovichev et al. 2004, 2006; Siidra et al. 2011). Within this approach, each OPb_4 tetrahedron is symbolized by a square. Each square is labeled by the number that corresponds to the number of the O site at the center of the tetrahedron. The [OPb] layer in litharge thus corresponds to the 2-dimensional (2-D) layer of squares (Table 1) that fill the 2-D plane without gaps and overlaps. In turn, tetrahedral layers in the PbO derivative structures correspond to two dimensional arrangements of black and white squares, where the latter symbolize vacancies. The topological function of a tetrahedron within the layer can be visualized by investigation of the local coordination of a given square by the adjacent squares, i.e., by all squares with which it has common points. The arrangement of black squares around the central square p is its first corona, $c^1(p)$ (Krivovichev et al. 1997a, b). The second corona, $c^2(p)$, is as a set of black squares that surround the first corona, and so on. Since the $[O_{21}Pb_{32}]^{22+}$ layer in hereroite consists of modules of the symesite- and kombatite-type

194 layers, these layers are analyzed first in order to understand topological relationships between the three
195 minerals.

196 Figure 5a shows the 2-D array of squares that represents the arrangement of OPb_4 tetrahedra
197 within the $[O_7Pb_{10}]^{6+}$ block in the structure of symesite. The following pairs of tetrahedra have identical
198 first coronas: $O5Pb_4$ and $O11Pb_4$, $O6Pb_4$ and $O10Pb_4$, and $O8Pb_4$ and $O9Pb_4$. The $O7Pb_4$ tetrahedron
199 has a unique arrangement and therefore its topological function is unique, even from the viewpoint of
200 the first-order analysis (Fig. 5c). To further investigate topological functions of different tetrahedra, one
201 has to examine their higher-order configurations (Fig. 5e). The analysis shows that, within the above
202 mentioned pairs, tetrahedra have the same topological functions, despite the fact that they are non-
203 equivalent crystallographically. The topological symmetry of the $[O_7Pb_{10}]^{6+}$ block in symesite is
204 therefore lower than its crystallographic symmetry.

205 The 2-D array of oxocentered tetrahedra within the $[O_9Pb_{14}]^{8+}$ layer in the structures of
206 kombatite and sahlinite, and the schemes of the first coronas for all six symmetrically independent
207 tetrahedra in the structure are shown in Figures 5b and d, respectively. The $O1Pb_4$-$O3Pb_4$ pair and the
208 $O7Pb_4$-$O8Pb_4$ pair have identical first coronas. However, their second coronas are different, and
209 therefore all symmetry-independent OPb_4 tetrahedra have different topological functions.

210 As the $[O_{21}Pb_{32}]^{22+}$ layer in the structure of hereroite consists of both kombatite and symesite
211 modules, it can be expected that its topological structure is more complex than that of the parent
212 structures (Fig. 6). The analysis of square lattice shows that it is the case indeed. For instance, the O10-
213 , O11-, O14-, O15-, O17-, and O19-centered OPb_4 tetrahedra have the same first coronas. Analysis of
214 the second-order configurations shows that O15- and O19-centered tetrahedra possess unique second
215 coronas, whereas, for the rest the second coronas are identical. The O10-, O11-, O14-, and O17-
216 centered OPb_4 tetrahedra can be distinguished by their third coronas only, which means that their
217 topological functions are unique. The O18- and O20-centered tetrahedra display even more complex
218 behaviour, since they can be distinguished by their fourth coronas only. In general, all symmetry-
219 independent OPb_4 tetrahedra in hereroite are unique in their global topological properties.

The most striking feature of the structure of hereroite is the combination of the kombatite and symesite modules arranged within one structural unit. Recently, modular approach to the structures of complex inorganic phases attracted considerable attention (see, e.g. Ferraris et al. 2004) and proved to be the useful concept for rational design of novel families of inorganic compounds (Kabbour et al. 2006). The structure of hereroite shows that this approach is also operational for complex Pb oxyhalide phases accommodating tetrahedral anions of slightly different size (e.g. silicate and arsenate). The observed dependence of the topology of the O-Pb layer upon the size of tetrahedral anionic species is remarkable and may be used for preparation of new layered inorganic compounds with novel structural architectures.

Acknowledgements

This work was supported by the President of Russian Federation grant for young scientists (# MK-5074.2011.5), RFBR-DFG collaboration research grant and the SPbSU X-ray Diffraction Resource center.

References cited

Aurivillius, B. (1982) On the crystal structure of a number of non-stoichiometric mixed lead oxide halides composed of PbO like blocks and single halogen layers. Chemica Scripta, 19, 97-107.

Aurivillius, B. (1983) On the crystal structure of some non-stoichiometric mixed lead oxide halides and their relation to the minerals "lorettoite" and sundiusite. Chemica Scripta, 22, 51-61.

Boher, P., Garnier, P., Gavarri, J.R., and Hewat, A.W. (1985) Monoxyde quadratique PbO: Description de la transition structurale ferroelastique. Journal of Solid State Chemistry, 57, 343-350.

Bonaccorsi, E., and Pasero, M. (2003) Crystal structure refinement of sahlinite, $Pb_{14}(AsO_4)_2O_9Cl_4$. Mineralogical Magazine. 67, 15-21.

Brown, I.D., and Altermatt, D. (1985) Bond-valence parameters obtained from a systematic analysis of the Inorganic Crystal Structure Database. Acta Crystallographica, B41, 244-247.

Cairncross, B. (1997) The Otavi Mountainland Cu-Pb-Zn-V deposits of Namibia. Mineralogical Record, 28, 109-113.

Chen, X., Song, F., Chang, X., Zang, H., and Xiao, W. (2009) Syntheses and characterization of two oxoborates, $(Pb_3O)_2(BO_3)_2MO_4$ (M = Cr, Mo). Journal of Solid State Chemistry, 182, 3091-3097.

Cooper, M.A., and Hawthorne, F.C. (1994) The crystal structure of kombatite, $Pb_{14}(VO_4)_2O_9Cl_4$, a complex heteropolyhedral sheet mineral. American Mineralogist, 79, 550-554.

Cziczo, D.J., Stetzer, O., Worringen, A., Ebert, M., Weinbruch, S., Kamphus, M., Gallavardin, S.J., Curtius, J., Borrmann, S., Froyd, K.D., Mertes, S., Möhler, O., Lohmann, U. (2009) Inadvertent climate modification due to anthropogenic lead. Nature Geoscience, 2, 333-336.

Dunn, P.J., and R.C. Rouse (1980) Sundiusite, a new lead sulfate oxychloride from Långban, Sweden. American Mineralogist, 65, 506–508.

Endara, D., Colmont, M., Huve, M., Tricot, G., Carpentier, L., and Mentre, O. (2012) Novel tailormade $Bi_4MO_4(PO_4)_2$ structural type (M = Mg, Zn). Inorganic Chemistry, 51, 4438-4447.

Ferraris, G., Makovicky, E., and Merlino, S. (2004) Crystallography of Modular Materials. Oxford University Press, Oxford.

Huvé, M., Colmont, M., Lejay, J., Aschehoug, P., and Mentré, O. (2009) Building units and intergrowths: toward the design of an extended family of acentric Bi-Based materials with second harmonic generacy. Chemistry of Materials, 21, 4019-4029.

Kabbour, H., Cario, L., Danot, M., and Meerschaut, A. (2006) Design of a new family of inorganic compounds $Ae_2F_2SnX_3$ (Ae = Sr, Ba; X = S, Se) using rock salt and fluorite 2D building blocks. Inorganic Chemistry, 45, 917-922.

Kampf, A.R.. Mills, S.J., and Pinch, W. (2011) Plumboselite, $Pb_3O_2(SeO_3)$, a new oxidation-zone mineral from Tsumeb, Namibia. Mineralogy and Petrology, 101, 75-80.

Krivovichev, S.V. and Brown, I.D. (2001) Are the compressive effects of encapsulation an artifact of the bond valence parameters? Zeitschrift für Kristallographie, 216, 245-247.

Krivovichev, S.V., and Burns, P.C. (2001a) Crystal chemistry of lead oxide chlorides. I. Crystal structures of synthetic mendipite, $Pb_3O_2Cl_2$, and synthetic damaraite, $Pb_3O_2(OH)Cl$. European Journal of Mineralogy, 13, 801-809.

Krivovichev, S.V., and Burns, P.C. (2001b) Crystal structure of $Pb_3O_2(OH)Br$, a Br-analogue of damaraite. Solid State Sciences, 3, 455-459.

Krivovichev, S.V., and Burns, P.C. (2002) Crystal chemistry of lead oxide chlorides. II. Crystal structure of $Pb_7O_4(OH)_4Cl_2$. European Journal of Mineralogy, 14, 135-139.

Krivovichev, S.V., and Burns, P.C. (2006) The crystal structure of blixite $Pb_8O_5(OH)_2Cl_4$, a synthetic analogue of blixite? Canadian Mineralogist, 44, 515-522.

Krivovichev, S.V., and Filatov, S.K. (1999a) Structural principles for minerals and inorganic compounds containing anion-centered tetrahedra. American Mineralogist, 84, 1099-1106.

Krivovichev, S.V., and Filatov, S.K. (1999b) Metal arrays in structural units based on anion-centered metal tetrahedra. Acta Crystallographica, B55, 664-676.

Krivovichev, S. V., Armbruster, T., and Depmeier, W. (2004) Crystal structures of $Pb_8O_5(AsO_4)_2$ and $Pb_5O_4(CrO_4)$, and review of PbO-related structural units in inorganic compounds Journal of Solid State Chemistry, 177, 1321-1332.

Krivovichev, S. V., Siidra, O. I., Nazarchuk, E. V., Burns, P. C., and Depmeier, W. (2006) Exceptional topological complexity of lead oxide blocks in $Pb_{31}O_{22}X_{18}$ (X=Br, Cl). Inorganic Chemistry, 45, 3846-3848.

Krivovichev, S.V., Turner, R., Rumsey, M., Siidra, O.I., and Kirk, C.A. (2009) The crystal structure of mereheadite. Mineralogical Magazine, 73, 75-89.

Li, J., Pan, S., Zhao, W., Tian, X., Han, J., and Fan, X. (2011) Synthesis and crystal structure of a novel boratotungstate: $Pb_6B_2WO_{12}$. Solid State Sciences, 13, 966-969.

Matsumoto, H., Miyake, T., and Iwahara, H. (2001) Chloride ion conduction in $PbCl_2$-PbO system. Materials Research Bulletin, 36, 1177-1184.

Mauck, C.M., van den Heuvel, T.W.P., Hull, M.M., Zeller, M., and Oertel, C.M. (2010) Synthesis and structures of $Pb_3O_2(CH_3COO)_2 \cdot 0.5H_2O$ and $Pb_2O(HCOO)_2$: two corrosion products. Inorganic Chemistry, 49, 10736-10743.

Nagashima, M., and Armbruster, T. (2010) Ardennite, tiragalloite and medaite: structural control of $(As^{5+},V^{5+},Si^{4+})O_4$ tetrahedra in silicates. Mineralogical Magazine, 74, 55-71.

Noren, L., Tan, E.S.Q., Withers, R.L., Sterns, M., and Rundlof, H. (2002) A neutron, X-ray and electron diffraction study of the structures of $Pb_3O_2X_2$ (X=Cl, Br). Materials Research Bulletin, 37, 1431-1442.

O'Keeffe, M., and Hyde, B.G. (1996) Crystal Structures. I. Patterns and Symmetry. Mineralogical Society of America, Washington D.C.

Pfitzner, A., and Pohla, P. (2009) Syntheses and crystal structures of $PbSbO_2Br$, $PbSbO_2I$, and $PbBiO_2Br$. Zeitschrift für Anorganische und Allgemeine Chemie, 635, 1157-1159.

Post, J.E., and Buseck, P.R. (1985) Quantitative energy-dispersive analysis of lead halide particles from the Phoenix urban aerosol. Environmental Science and Technology, 19, 682-685.

Reshak, A.H., Chen, X., Auluck, S., and Kamarudin, H. (2012) Linear optical susceptibilities of the oxoborate $(Pb_3O)_2(BO_3)_2WO_4$: theory and experiment. Journal of Materials Science, 47, 5794-5800.

Rouse, R.C., Peacor, D.R., Dunn, P.J., Criddle, A.J., Stanley, C.J., and Innes, J. (1988) Asisite, a silicon-bearing lead oxychloride from the Kombat mine, South West Africa (Namibia). American Mineralogist, 73, 643-650.

Sheldrick, G.M. (2008) A short history of SHELX. Acta Crystallographica, A64, 112-122.

Sigman, N.B., and Korgel, B.A. (2005) Strongly birefringent $Pb_3O_2Cl_2$ nanobelts. Journal of American Chemical Society, 127, 10089-10095.

Siidra, O. I., Krivovichev, S. V., Armbruster, T., and Depmeier, W. (2007a) Lead rare-earth oxyhalides: syntheses and characterization of Pb_6LaO_7X (X = Cl, Br). Inorganic Chemistry, 46, 1523-1525.

Siidra, O. I., Krivovichev, S.V., and Depmeier, W. (2007b) Structure and mechanism of the ionic conductivity of the nonstoichiometric compound $Pb_{2+x}OCl_{2+2x}$. Doklady Physical Chemistry, 414, 128- 131.

Siidra, O. I., Krivovichev, S.V., and Depmeier, W. (2007c) Crystal chemistry of natural and synthetic lead oxyhalides. I. Crystal structure of $Pb_{13}O_{10}Cl_6$. Geology of Ore Deposits, 49, 827-834.

Siidra, O. I., Krivovichev, S.V., Turner, R., and Rumsey, M. (2008a) Chloroxiphite $Pb_3CuO_2(OH)_2Cl_2$: structure refinement and description in terms of oxocentered OPb_4 tetrahedra. Mineralogical Magazine, 72, 793-798.

Siidra, O. I., Krivovichev, S. V., Armbruster, T., and Depmeier, W. (2008b) Crystal chemistry of the mendipite-type system $Pb_3O_2Cl_2$ - $Pb_3O_2Cl_2$. Zeitschrift für Kristallographie, 223, 204-211.

Siidra, O.I., Krivovichev, S.V. and Filatov, S.K. (2008c) Minerals and synthetic Pb(II) compounds with oxocentered tetrahedra: review and classification. Zeitschrift für Kristallographie, 223, 114-126.

Siidra, O.I., Krivovichev, S.V., Turner, R.W., and Rumsey, M.S. (2011) Natural and synthetic layered oxyhalides. In: Krivovichev, S.V. (ed) Minerals as Advanced Materials II. Springer: Heidelberg New York Dordrecht London, pp. 319-332.

Siidra, O.I., Krivovichev, S.V., Turner, R.W., Rumsey, M.S., and Spratt, J. (2012) Crystal chemistry of layered Pb oxychloride minerals with PbO-related structures. II. Crystal structure of vladkrivovichevite, $[Pb_{32}O_{18}][Pb_4Mn_2O]Cl_{14}(BO_3)_8{\cdot}2H_2O$. American Mineralogist, submitted.

Symes, R.F., Cressey, G., Criddle, A.J., Stanley, C.J., Francis, J.G., and Jones, G.C. (1994) Parkinsonite, (Pb, Mo, □)$_8O_8Cl_2$, a new mineral from Merehead Quarry, Somerset. Mineralogical Magazine, 58, 59-68.

Turner, R.W. (2006). A mechanism for the formation of the mineralised manganese deposits at Merehead Quarry, Cranmore, Somerset, England. Mineralogical Magazine, 70, 629-653.

Turner, R.W, and Rumsey, M.S. (2010) Mineral relationships in the Mendip Hills. Journal of the Russell Society, 13, 3-47.

Turner, R., Siidra, O.I., Rumsey, M.S., Krivovichev, S.V., Stanley, C.J., Spratt, J. (2012a) Hereroite and vladkrivovichevite – two novel lead oxychlorides from the Kombat mine, Namibia. Mineralogical Magazine, accepted.

Turner, R., Siidra, O.I., Krivovichev, S.V., Stanley, C.J., Spratt, J. (2012b) Rumseyite, $[Pb_2OF]Cl$, the first naturally occurring fluoroxychloride mineral with the parent crystal structure for layered lead oxychlorides. Mineralogical Magazine, submitted.

Wan, G., Wang, G., Feng, F., and Yu, W. (2011) Synthesis and optical properties of elliptic Pb(OH)Br microdiskettes. Materials Research Bulletin, 46, 487-491.

Welch, M.D., Schofield, P.F., Cressey, G., and Stanley, C.J. (1996) Cation ordering in lead-molybdenum-vanadium oxychlorides. American Mineralogist, 81, 1350-1359

Welch, M.D., Criddle, A.J., and Symes, R.F. (1998) Mereheadite, $Pb_2O(OH)Cl$: a new litharge-related oxychloride from Merehead Quarry, Cranmore, Somerset. Mineralogical Magazine. 62, 387-393.

Welch, M.D., Cooper, M.A., Hawthorne, F.C., and Criddle, A.J. (2000) Symesite, $Pb_{10}(SO_4)O_7Cl_4(H_2O)$, a new PbO-related sheet mineral: description and crystal structure. American Mineralogist, 85, 1526-1533.

Welch, M.D., Hawthorne, F.C., Cooper, M., and Kyser, T.K. (2001) Trivalent iodine in the crystal structure of schwartzembergite, $Pb^{2+}{}_5I^{3+}O_6H_2Cl_3$. Canadian Mineralogist, 39, 785-795.

Walsh, A., Payne, D.J., Egdell, R.G., and Watson, G.W. (2011) Stereochemistry of post-transition metal oxides: revision of the classical lone pair model. Chemical Society Reviews, 40, 4455-4463.

373 **Figure Captions**

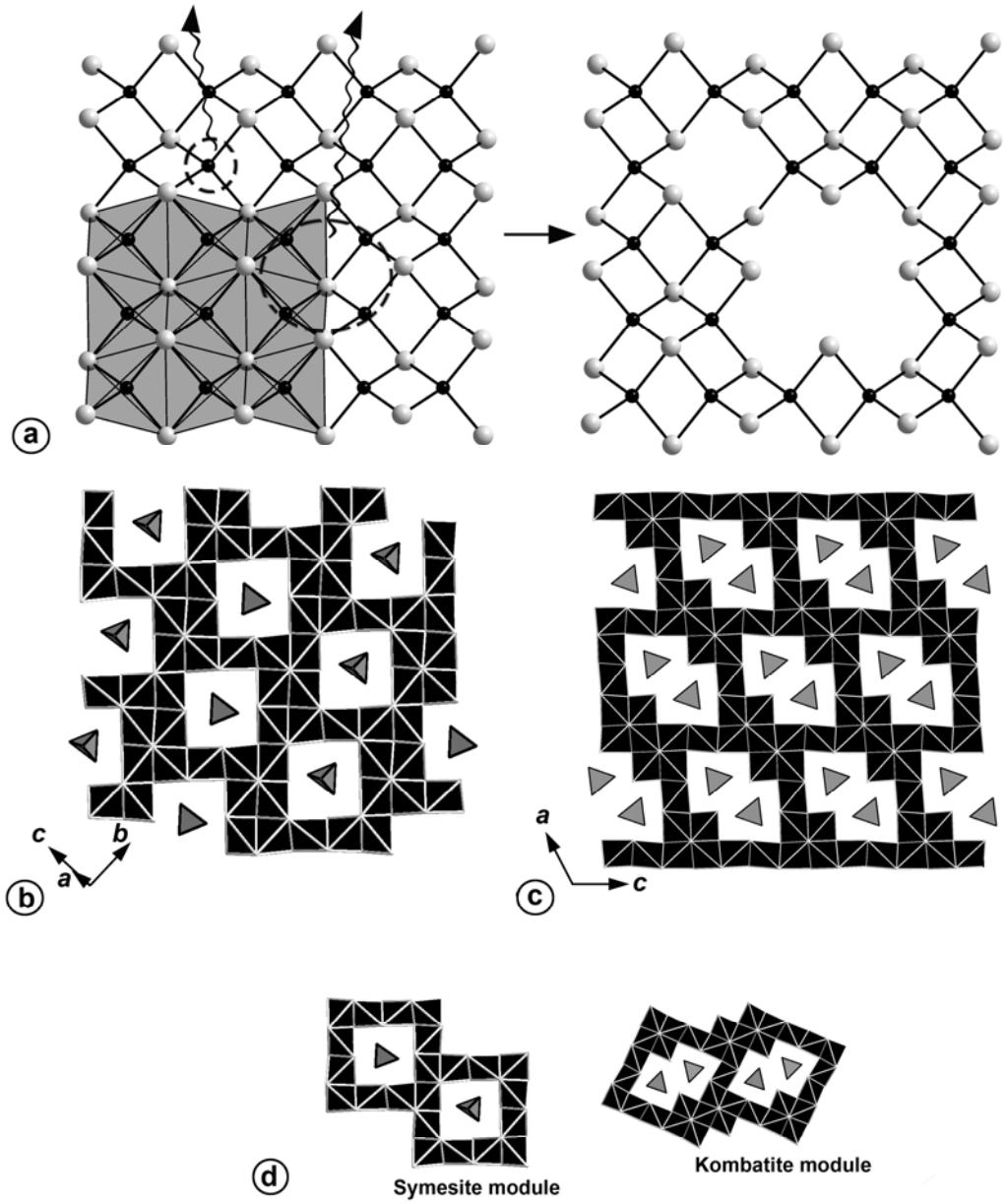

374

375 Figure 1. The [OPb] layer in litharge and formation of vacancies due to the removal of Pb and
376 O atoms (a); the $[O_7Pb_{10}]^{6+}$ layer in symesite shown as formed by edge-sharing OPb_4
377 tetrahedra with the square shaped vacancies occupied by the SO_4 anions (b); the $[O_9Pb_{14}]^{10+}$
378 layer in kombatite and sahlinite with the double square vacancies occupied by the VO_4 or
379 AsO_4 anions (c). Modules derived from the crystal structures of symesite and kombatite (d).

380

381

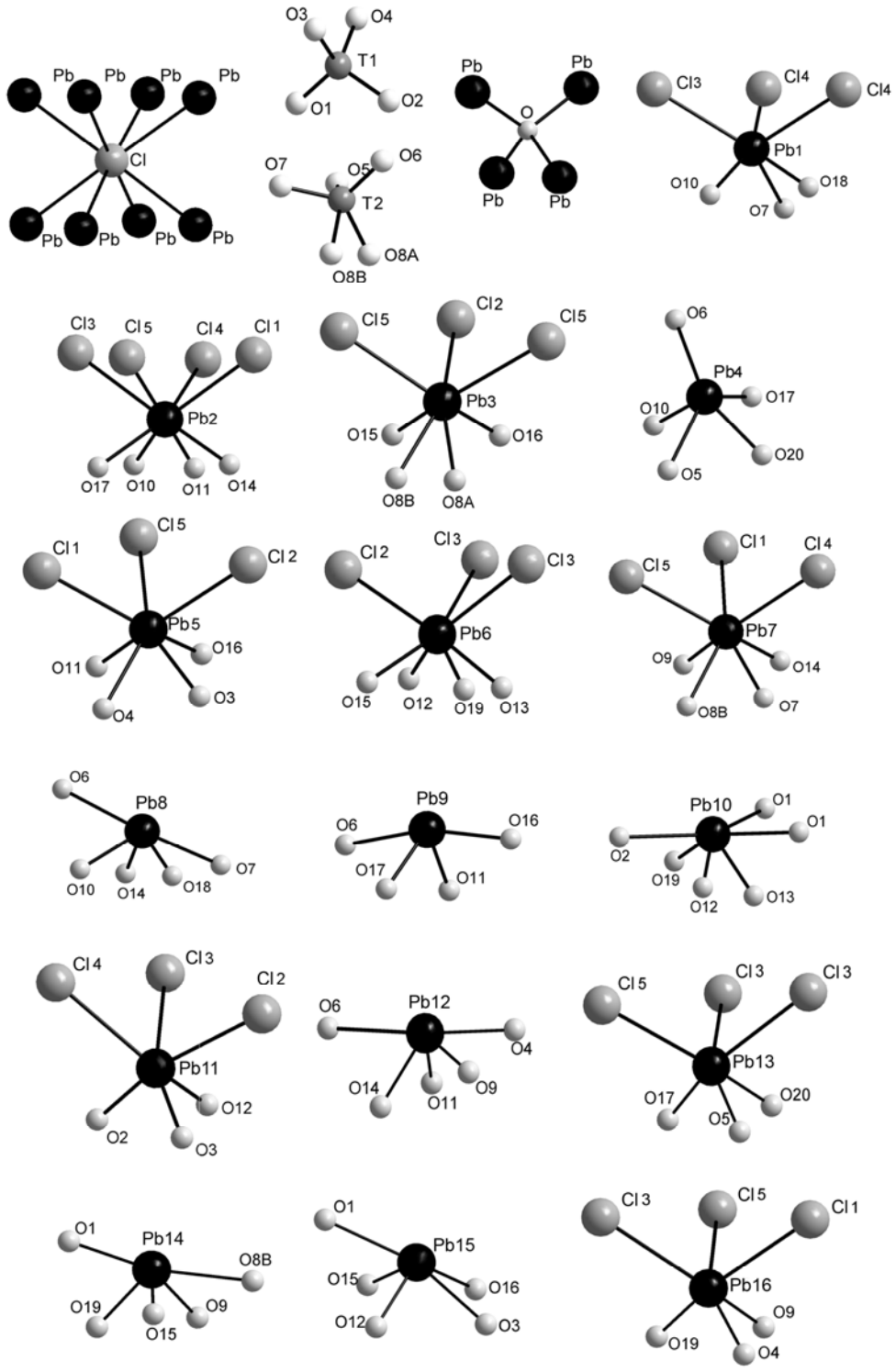

382

383 Figure 2. Coordination of atoms in the crystal structure of hereroite.

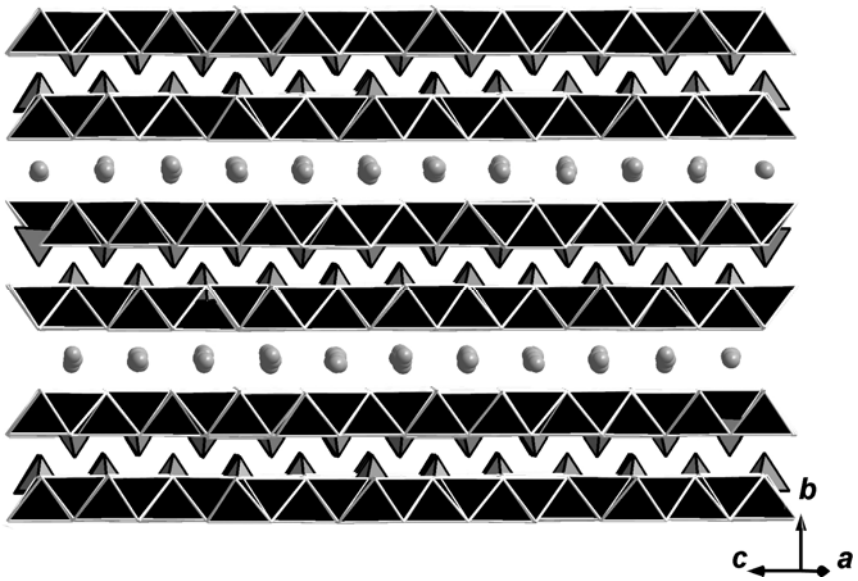

Figure 3. Projection of the crystal structure of hereroite along the extension of the PbO-type layers. Legend: OPb_4 tetrahedra = dark, AsO_4 and TO_4 tetrahedra are grey, Cl atoms are shown as spheres.

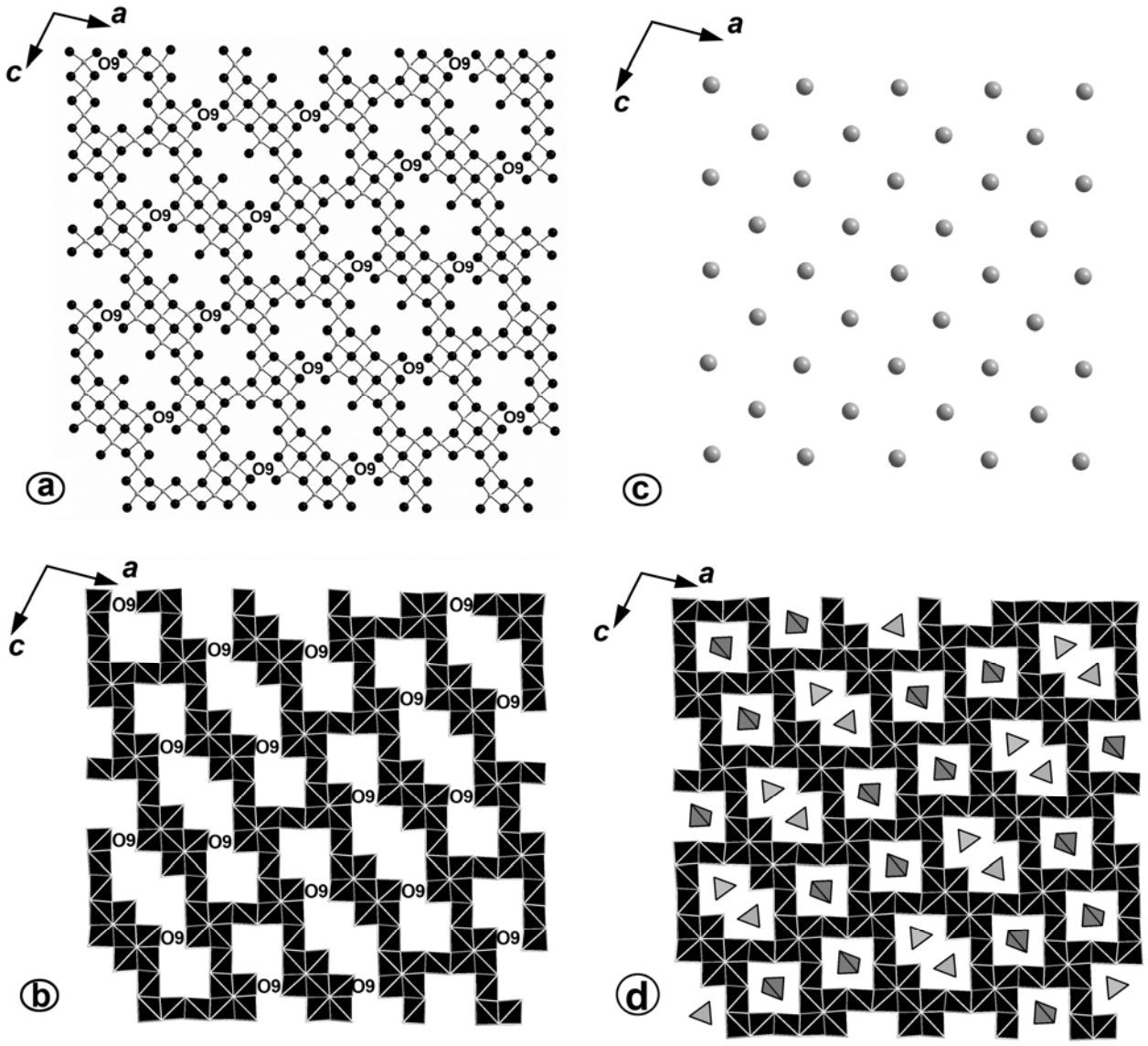

391

392

393 Figure 4. Ball-and-stick (a) and polyhedral (b) representations of the PbO-type layer in the

394 crystal structure of hereroite. Under-occupied O9 site is shown. The layer of Cl^- anions (c).

395 General projection of the $[O_{21}Pb_{32}]^{22+}$ layer with tetrahedral anions (d).

396

397

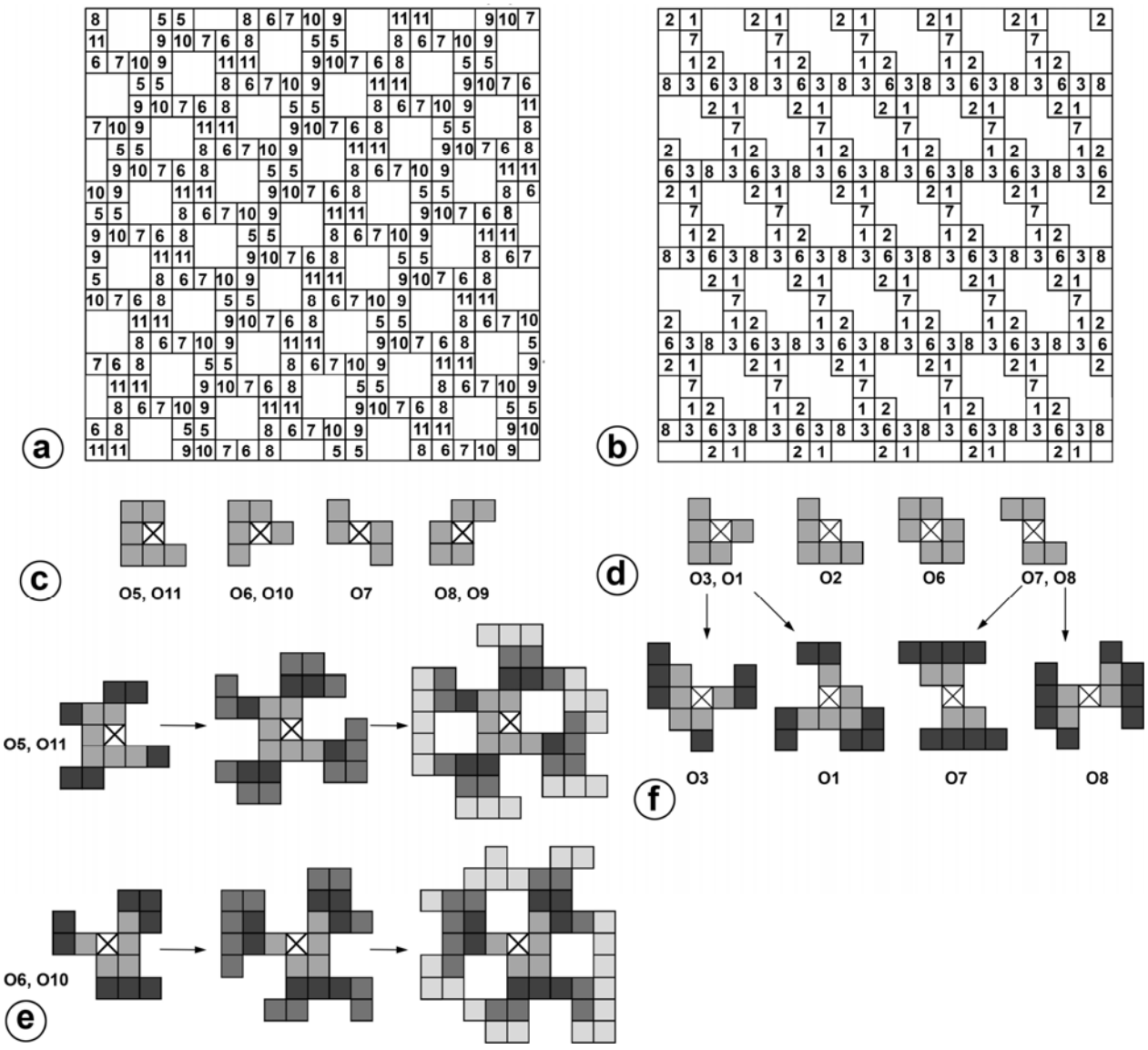

398

399 Figure 5. Topological structure of the $[O_7Pb_{10}]^{6+}$ layer in symesite (**a**) and the $[O_9Pb_{14}]^{8+}$ layer
400 in kombatite (**b**) examined using the method of square lattices: first coronas of the OPb_4
401 tetrahedra (central tetrahedra are shown as crossed squares) in the structures of symesite
402 and kombatite (**c, d**, respectively); second, third, and fourth coronas of the $O5Pb_4$, $O11Pb_4$,
403 $O6Pb_4$, and $O10Pb_4$ tetrahedra in symesite (**e**); second coronas of the $O1Pb_4$, $O3Pb_4$ $O7Pb_4$,
404 and $O8Pb_4$ tetrahedra in kombatite (**f**).

405

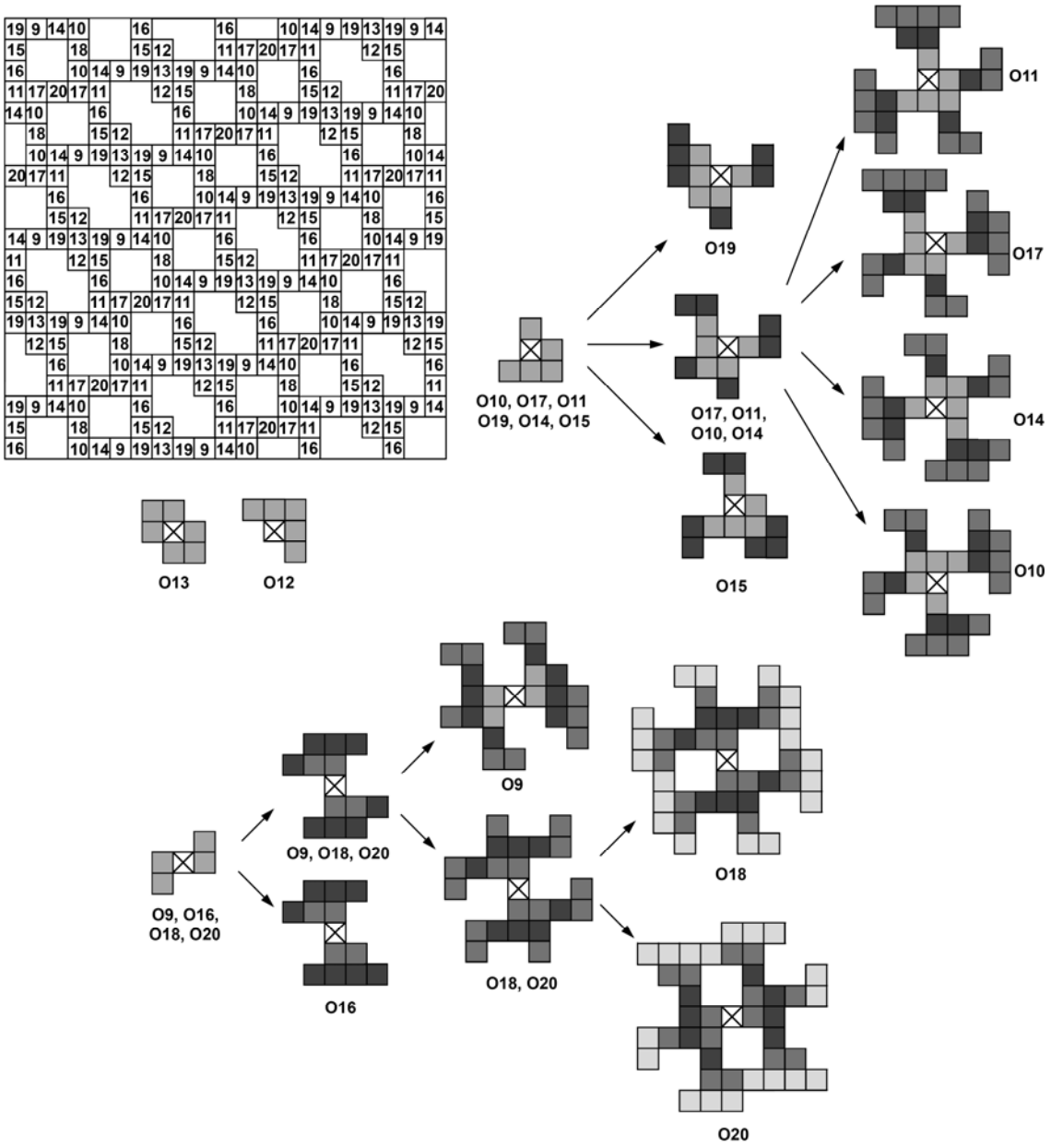

406

407 Figure 6. Topological structure of the $[O_{21}Pb_{32}]^{22+}$ layer in hereroite examined using the

408 method of square lattices. See the text for details.

409

410

411

412

413

414 **Table 1**. Crystallographic data for layered Pb oxychloride minerals with PbO-related structures
415

Mineral name	Chemical formula	Space group	*a* [Å] / *α* [deg]	*b* [Å] / *β* [deg]	*c* [Å] / *γ* [deg]	Ref.
Rumseyite	$(Pb_2OF)Cl$	*I*4/*mmm*	4.065 / 90	4.065 / 90	12.631 / 90	1
Blixite	$Pb_8O_5(OH)_2Cl_4$	*C*2/*c*	26.069 / 90	5.835 / 102.612	22.736 / 90	2
Symesite	$Pb_{10}(SO_4)O_7Cl_4(H_2O)$	$B\bar{1}$	19.727 / 82.21	8.796 / 78.08	13.631 / 100.04	3
Kombatite	$Pb_{14}(VO_4)_2O_9Cl_4$	*C*2/*c*	12.682 / 90	22.566 / 118.11	11.279	4
Sahlinite	$Pb_{14}(AsO_4)_2O_9Cl_4$	*C*2/*c*	12.704 / 90	22.576 / 118.37	11.287 / 90	5
Mereheadite	$Pb_{47}O_{24}(OH)_{13}Cl_{25}(BO_3)_2(CO_3)$	*Cm*	17.372 / 90	27.941 / 93.152	10.666 / 90	6
Hereroite	$[Pb_{32}O_{20}(O,\square)](AsO_4)_2$ $((Si,As,V,Mo)O_4)_2Cl_{10}$	*C*2/*c*	23.139 / 90	22.684 / 102.090(3)	12.389 / 90	7
Vladkrivovichevite	$[Pb_{32}O_{18}][Pb_4Mn_2O]$ $Cl_{14}(BO_3)_8{\cdot}2H_2O$	*Pmmn*	12.759/ 90	27.169 / 90	11.515 / 90	8
Sundiusite*	$Pb_{10}O_8(SO_4)Cl_2$	*C2/m, Cm, C*2	24.67 / 90	3.781 / 100.07	11.881 / 90	9

416 * structure unknown
417
418 References: (1) Turner et al. 2012b; (2) Krivovichev and Burns, 2006; (3) Welch et al. 2000; (4)
419 Cooper and Hawthorne 1994; (5) Bonaccorsi and Pasero 2003; (6) Krivovichev et al. 2009; (7) this
420 work; (8) Siidra et al. 2012; (9) Dunn and Rouse 1980.
421

422

423 **Table 2**. Crystallographic data and
424 refinement parameters for hereroite

a (Å)	23.139(4)
b (Å)	22.684(4)
c (Å)	12.389(2)
β (°)	102.090(3)
V (Å^3)	6358.8(18)
Space group	*C*2/*c*
Z	4
D_{calc}(g/cm^3)	8.144
μ (mm^{-1})	86.456
F_{000}	12748.2
Crystal size (mm)	0.11×0.10×0.08
Radiation	Mo*K*α
h_{min}, h_{max}	-38, 33
k_{min}, k_{max}	-37, 37
l_{min}, l_{max}	-20, 20
$2\theta_{min}$, $2\theta_{max}$	1.27, 36.15
Total Ref.	56375
Unique Ref.	14483
Unique $\|F_o\| \geq 4\sigma_F$	6931
R_1	0.054
wR_2	0.108
S	1.002

425 **Table 3**. Atomic coordinates, displacement parameters (Å^2), bond-valence sums* (valence units) and site-occupancy factors (SOFs) for hereroite
426

Atom	BVS	*x*	*y*	*z*	U_{eq}	U_{11}	U_{22}	U_{33}	U_{23}	U_{13}	U_{12}
Pb1	1.90	0.02370(3)	0.33013(3)	0.11179(5)	0.01240(13)	0.0127(3)	0.0114(3)	0.0122(3)	-0.0007(2)	0.0004(2)	0.0030(2)
Pb2	1.99	-0.13847(3)	0.33113(2)	-0.05572(5)	0.00938(10)	0.0116(2)	0.0066(2)	0.0097(2)	-0.0005(2)	0.00158(17)	-0.0008(2)
Pb3	2.17	0.24274(3)	0.16730(3)	0.00179(5)	0.01195(13)	0.0126(3)	0.0103(3)	0.0117(3)	0.0010(2)	-0.0002(2)	-0.0027(2)
Pb4	1.93	-0.03666(3)	0.55670(3)	0.37405(5)	0.01179(12)	0.0157(3)	0.0076(3)	0.0121(2)	-0.0009(2)	0.0032(2)	0.0037(2)
Pb5	1.88	-0.30232(3)	0.33470(3)	-0.22005(5)	0.01283(13)	0.0158(3)	0.0104(3)	0.0106(3)	0.0016(2)	-0.0010(2)	-0.0036(2)
Pb6	1.90	0.08073(2)	0.16427(2)	-0.17277(5)	0.00920(12)	0.0099(2)	0.0057(2)	0.0111(3)	0.0008(2)	0.00000(19)	-0.0001(2)
Pb7	1.95	-0.19191(3)	0.66864(3)	-0.28106(5)	0.01232(13)	0.0125(3)	0.0115(3)	0.0125(3)	-0.0048(2)	0.0016(2)	-0.0015(2)
Pb8	1.88	-0.07902(3)	0.44391(3)	0.15108(5)	0.01180(13)	0.0131(3)	0.0062(3)	0.0154(3)	-0.0033(2)	0.0014(2)	-0.0008(2)
Pb9	1.83	-0.19752(3)	0.44554(3)	-0.26142(5)	0.01285(13)	0.0136(3)	0.0076(3)	0.0175(3)	0.0046(2)	0.0035(2)	0.0017(2)
Pb10	1.86	-0.02290(3)	0.04875(3)	-0.11756(6)	0.01329(12)	0.0133(3)	0.0091(2)	0.0171(3)	0.0060(2)	0.0025(2)	-0.0008(2)
Pb11	1.87	0.03095(3)	0.16428(3)	0.11131(5)	0.01614(14)	0.0170(3)	0.0166(3)	0.0149(3)	-0.0063(3)	0.0034(2)	0.0028(3)
Pb12	1.91	-0.23979(3)	0.55461(3)	-0.48495(5)	0.01140(12)	0.0153(3)	0.0069(3)	0.0114(2)	0.0020(2)	0.0016(2)	-0.0016(2)
Pb13	1.83	-0.08201(3)	0.67123(3)	0.17201(5)	0.01177(12)	0.0133(3)	0.0097(3)	0.0125(3)	0.0035(2)	0.0030(2)	0.0019(2)
Pb14	1.96	0.18340(3)	0.05181(3)	-0.23282(5)	0.01399(13)	0.0170(3)	0.0115(3)	0.0126(3)	-0.0014(2)	0.0012(2)	0.0061(2)
Pb15	1.75	0.13716(3)	0.05425(3)	0.03687(5)	0.01445(13)	0.0137(3)	0.0092(3)	0.0205(3)	0.0069(2)	0.0036(2)	0.0025(2)
Pb16	1.78	0.14468(3)	0.16517(3)	-0.43715(5)	0.01309(12)	0.0142(3)	0.0117(3)	0.0146(3)	0.0041(2)	0.0056(2)	0.0026(2)
T1[$]	3.88	0.09489(10)	-0.06941(11)	-0.15611(18)	0.0129(6)	0.0111(11)	0.0172(12)	0.0104(10)	0.0015(8)	0.0024(7)	-0.0016(9)
As1	5.09	-0.13500(8)	0.56799(8)	-0.05413(16)	0.0174(5)	0.0179(9)	0.0133(9)	0.0225(9)	0.0010(8)	0.0076(7)	0.0004(7)
Cl1	0.92	-¼	¼	0	0.0207(14)	0.022(3)	0.024(4)	0.017(3)	0.003(2)	0.007(2)	0.004(2)
Cl2	0.66	0.1401(1)	0.2363(2)	0.0553(4)	0.0204(8)	0.016(1)	0.027(2)	0.016(1)	-0.002(2)	0.0005(14)	0.001(1)
Cl3	0.78	-0.0270(1)	0.24850(18)	-0.1112(4)	0.0215(10)	0.019(2)	0.028(3)	0.018(2)	-0.0065(19)	0.0047(17)	-0.002(1)
Cl4	0.89	-0.0782(1)	0.25894(19)	0.1645(3)	0.0192(9)	0.021(2)	0.0171(19)	0.017(2)	0.0032(16)	-0.0002(17)	0.001(1)
Cl5	0.79	-0.3020(1)	0.75128(19)	-0.2273(4)	0.0200(10)	0.018(2)	0.027(3)	0.015(2)	0.0006(17)	0.0044(17)	0.001(1)
O1	1.76	0.0926(6)	0.0011(6)	-0.1634(10)	0.030(3)						
O2	1.60	0.0413(5)	-0.0931(6)	-0.0975(11)	0.031(3)						
O3	1.71	-0.4013(5)	0.3997(5)	-0.2770(9)	0.016(2)						
O4	1.75	-0.3410(5)	0.4083(6)	-0.0730(10)	0.024(3)						
O5	1.88	-0.0749(9)	0.5950(9)	0.0400(16)	0.077(6)						
O6	1.97	-0.1331(5)	0.4952(6)	-0.0590(10)	0.027(3)						
O7	1.98	-0.1185(9)	0.5952(11)	-0.1698(18)	0.099(8)						
O8A[#]	1.94	-0.1839(14)	0.5906(15)	0.015(3)	0.071(12)						
O8B[£]	1.66	-0.2059(16)	0.5928(17)	-0.115(3)	0.048(13)						
O9[¶]	1.89	0.2278(5)	0.1153(5)	-0.3526(9)	0.008(3)						
O10	1.99	-0.0489(4)	0.3895(5)	0.0160(8)	0.014(2)						

O11	2.00	-0.2255(4)	0.3907(5)	-0.1289(8)	0.010(2)
O12	1.95	0.0560(4)	0.1105(5)	-0.0214(8)	0.012(2)
O13	2.10	0	0.1031(6)	-¼	0.006(3)
O14	2.02	-0.1587(4)	0.3887(5)	0.0934(9)	0.014(2)
O15	2.01	0.1695(4)	0.1091(5)	-0.0956(8)	0.011(2)
O16	1.86	0.2221(5)	0.1126(5)	0.1404(9)	0.018(3)
O17	1.98	-0.1172(4)	0.3897(5)	-0.2119(9)	0.015(2)
O18	1.90	0	0.3853(7)	¼	0.013(3)
O19	1.96	0.1077(4)	0.1034(5)	-0.3268(8)	0.012(2)
O20	1.94	0	0.6202(7)	¼	0.015(3)

* calculated using bond-valence parameters from Krivovichev and Brown (2001) for the Pb^{2+}-O bonds and from Brown and Altermatt (1985) for other bonds (bond-valences for the T-O bonds calculated using the Si^{4+}-O bond-valence parameters)

$ $Si_{0.48}As_{0.28}V_{0.16}Mo_{0.08}$ Note: assigned on the basis of chemical data.

S.O.F. = 0.58(3)

£ S.O.F. = 0.42(3)

¶ S.O.F. = 0.85(3)

433 **Table 4**. Selected bond lengths (Å) in the structure of hereroite
434

Pb1-O18	2.279(8)	Pb7-O9	2.239(11)	Pb14-O15	2.215(10)
Pb1-O10	2.281(10)	Pb7-O14	2.281(11)	Pb14-O19	2.223(10)
Pb1-O7	2.74(2)	Pb7-O7	2.56(2)	Pb14-O9	2.444(12)
Pb1-O5	2.96(2)	Pb7-O8B	2.75(4)	Pb14-O1	2.690(13)
Pb1-Cl4	3.040(5)	Pb7-Cl4	3.289(4)	Pb14-O8B	2.83(4)
Pb1-Cl4	3.228(4)	Pb7-Cl1	3.3232(7)		
Pb1-Cl3	3.329(4)	Pb7-Cl5	3.341(4)	Pb15-O12	2.260(10)
				Pb15-O15	2.306(11)
Pb2-O14	2.389(11)	Pb8-O14	2.220(10)	Pb15-O16	2.491(11)
Pb2-O11	2.437(10)	Pb8-O10	2.303(11)	Pb15-O1	2.757(12)
Pb2-O10	2.463(10)	Pb8-O18	2.382(8)	Pb15-O3	2.839(11)
Pb2-O17	2.480(11)	Pb8-O7	2.72(2)		
Pb2-Cl4	3.236(4)	Pb8-O6	2.886(12)	Pb16-O19	2.248(11)
Pb2-Cl4	3.295(4)			Pb16-O9	2.287(11)
Pb2-Cl1	3.3570(7)	Pb9-O17	2.227(10)	Pb16-O4	2.440(12)
Pb2-Cl5	3.373(5)	Pb9-O11	2.259(11)	Pb16-Cl5	3.279(4)
		Pb9-O16	2.393(11)	Pb16-Cl1	3.3231(7)
Pb3-O16	2.250(12)	Pb9-O6	2.866(12)	Pb16-Cl3	3.468(5)
Pb3-O15	2.284(10)	Pb9-O8A	2.96(3)		
Pb3-O8A	2.41(3)			T1-O1	1.60(1)
Pb3-O8B	2.66(4)	Pb10-O13	2.204(7)	T1-O2	1.65(1)
Pb3-Cl2	3.030(5)	Pb10-O19	2.302(10)	T1-O3	1.67(1)
Pb3-Cl5	3.390(4)	Pb10-O12	2.410(10)	T1-O4	1.69(1)
Pb3-Cl5	3.395(4)	Pb10-O2	2.961(13)		
		Pb10-O1	3.044(13)	As1-O8A	1.64(3)
Pb4-O10	2.207(11)	Pb10-O1	3.049(12)	As1-O6	1.65(1)
Pb4-O17	2.292(10)			As1-O7	1.68(2)
Pb4-O20	2.388(9)	Pb11-O12	2.220(11)	As1-O5	1.72(1)
Pb4-O5	2.721(19)	Pb11-O2	2.306(13)	As1-O8B	1.75(4)
Pb4-O6	2.798(13)	Pb11-O3	2.359(10)		
		Pb11-Cl2	3.205(5)		
Pb5-O16	2.269(12)	Pb11-Cl3	3.392(5)		
Pb5-O11	2.283(10)	Pb11-Cl4	3.482(4)		
Pb5-O3	2.691(10)				
Pb5-O4	2.756(13)	Pb12-O11	2.253(10)		
Pb5-Cl5	3.239(4)	Pb12-O14	2.313(10)		
Pb5-Cl2	3.250(4)	Pb12-O9	2.380(12)		
Pb5-Cl1	3.3476(7)	Pb12-O4	2.513(11)		
		Pb12-O6	3.026(13)		
Pb6-O13	2.363(8)				
Pb6-O12	2.404(10)	Pb13-O20	2.260(8)		
Pb6-O15	2.425(10)	Pb13-O17	2.265(11)		
Pb6-O19	2.536(10)	Pb13-O5	2.41(2)		
Pb6-Cl2	3.304(5)	Pb13-Cl3	3.273(5)		
Pb6-Cl3	3.311(4)	Pb13-Cl3	3.324(5)		
Pb6-Cl3	3.354(5)	Pb13-Cl5	3.396(4)		

435
436
437
438

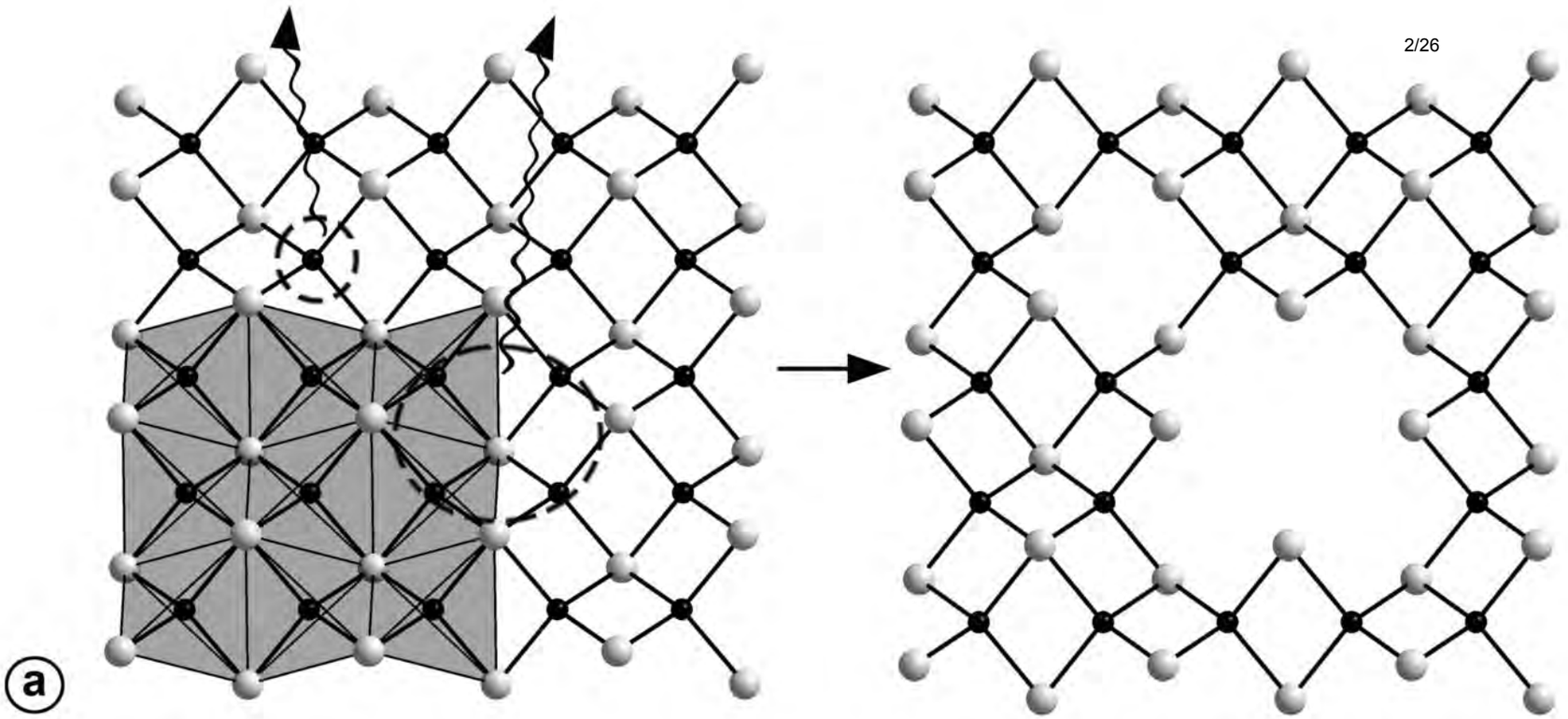
a

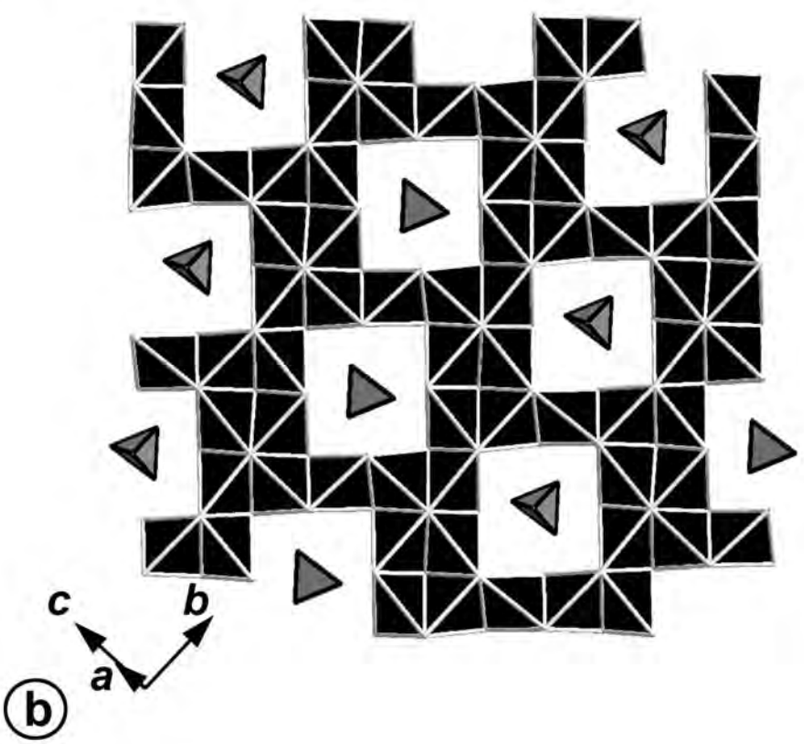
c
b
a
b

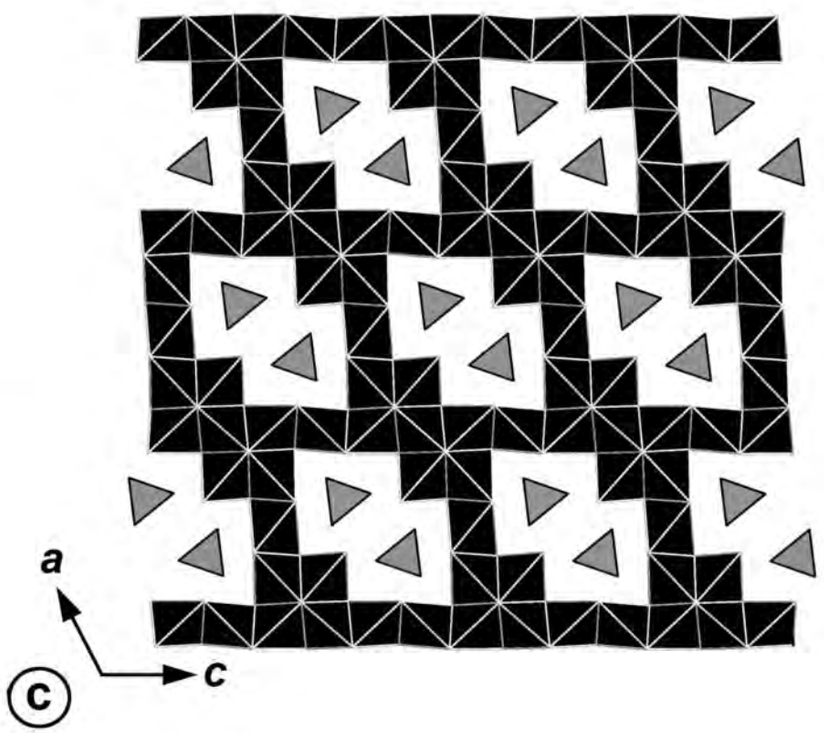
a
c
c

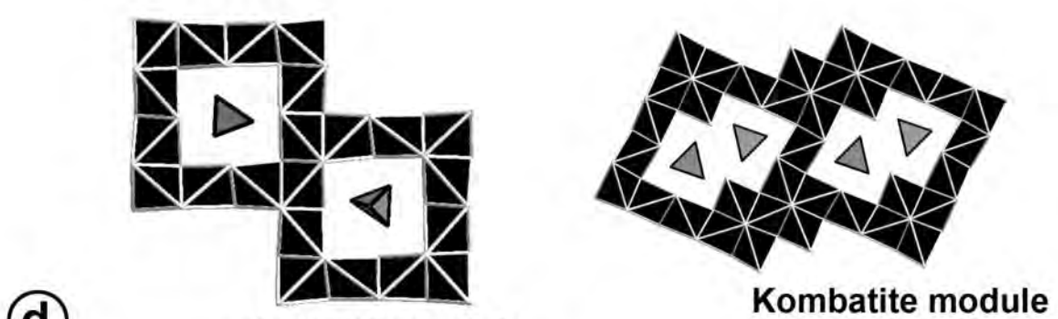
d
Symesite module
Kombatite module

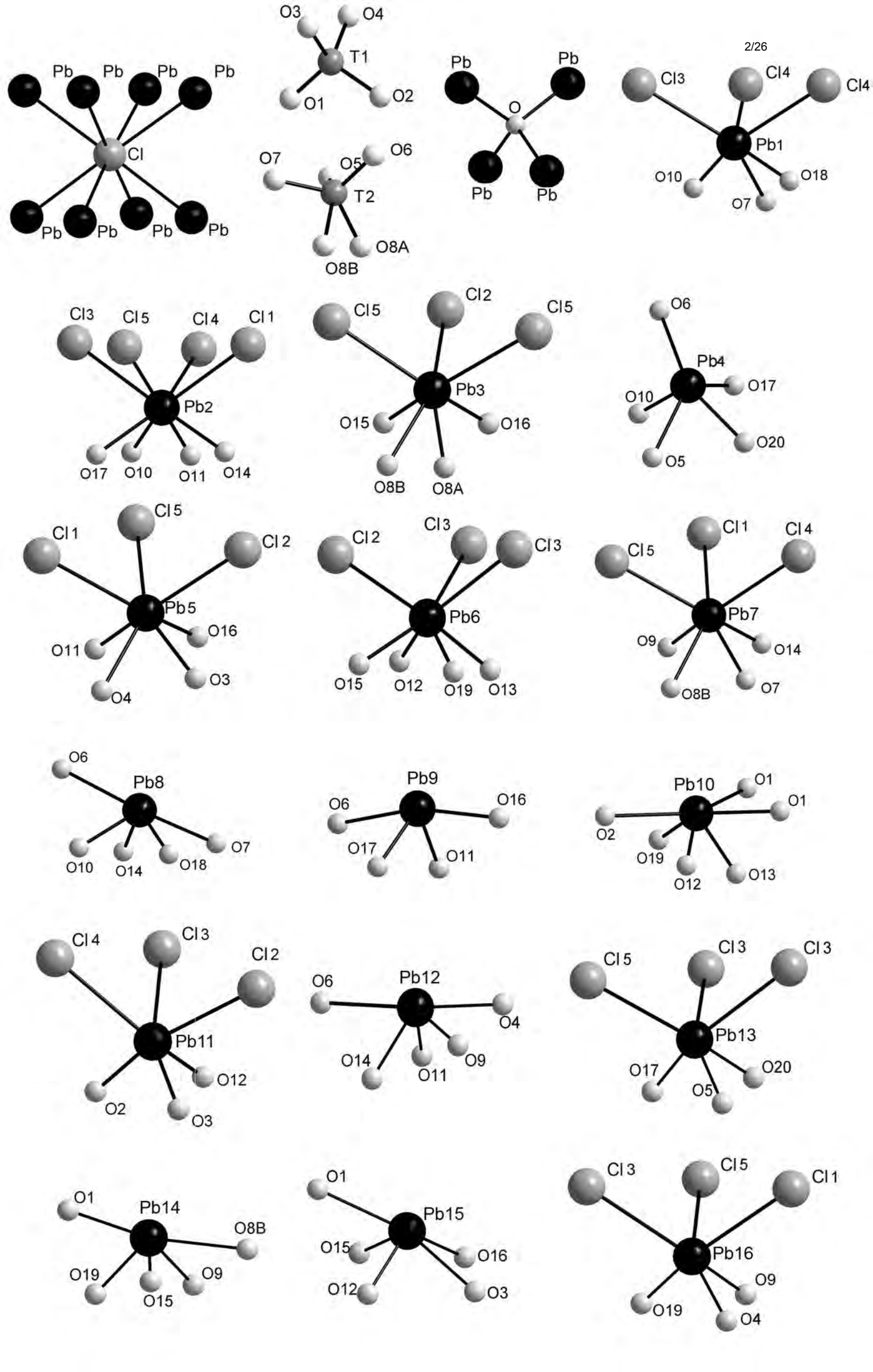
Pb
Pb
Pb
Pb
Cl
Pb
Pb
Pb
Pb
O3
O4
T1
O1
O2
O7
O5
O6
T2
O8A
O8B
Pb
Pb
O
Pb
Pb
Cl3
Cl4
Cl4
Pb1
O10
O18
O7
Cl3
Cl5
Cl4
Cl1
Pb2
O17
O10
O11
O14
Cl5
Cl2
Cl5
Pb3
O15
O16
O8B
O8A
O6
Pb4
O17
O10
O20
O5
Cl1
Cl5
Cl2
Pb5
O16
O11
O3
O4
Cl2
Cl3
Cl3
Pb6
O15
O12
O19
O13
Cl1
Cl4
Cl5
Pb7
O9
O14
O8B
O7
O6
Pb8
O10
O14
O18
O7
Pb9
O6
O16
O17
O11
Pb10
O1
O1
O2
O19
O12
O13
Cl4
Cl3
Cl2
Pb11
O12
O2
O3
O6
Pb12
O4
O14
O11
O9
Cl5
Cl3
Cl3
Pb13
O17
O20
O5
O1
Pb14
O8B
O19
O9
O15
O1
Pb15
O15
O16
O12
O3
Cl3
Cl5
Cl1
Pb16
O9
O19
O4

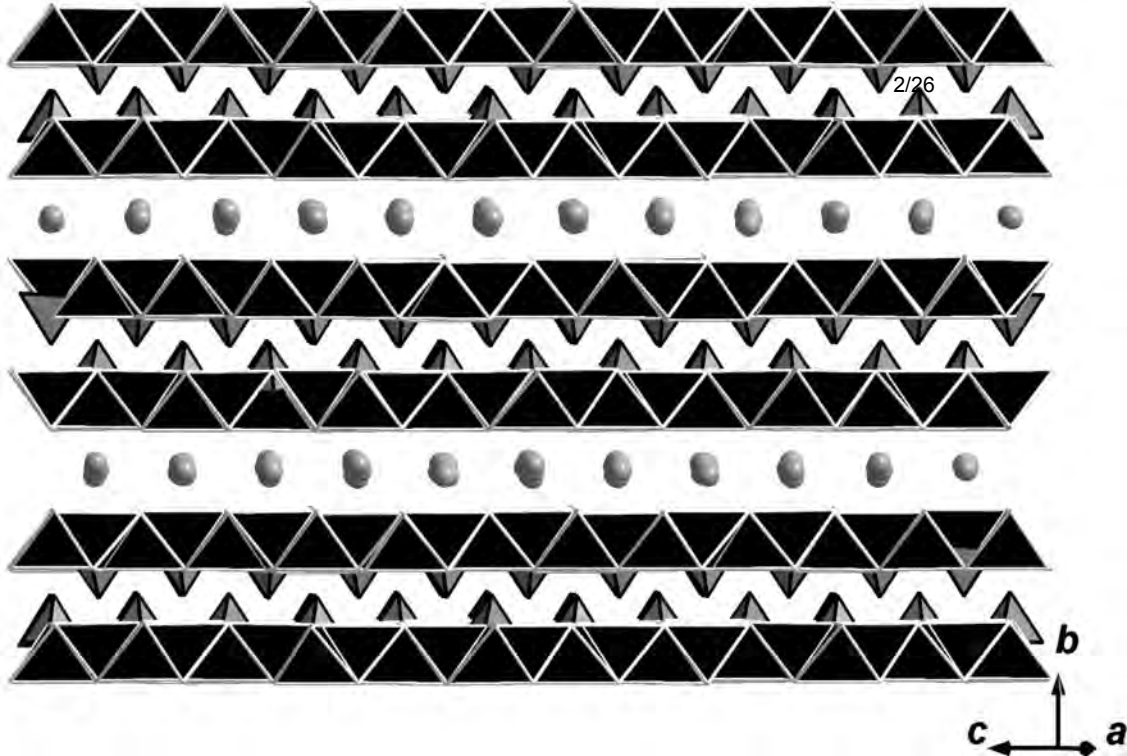
b
c
a

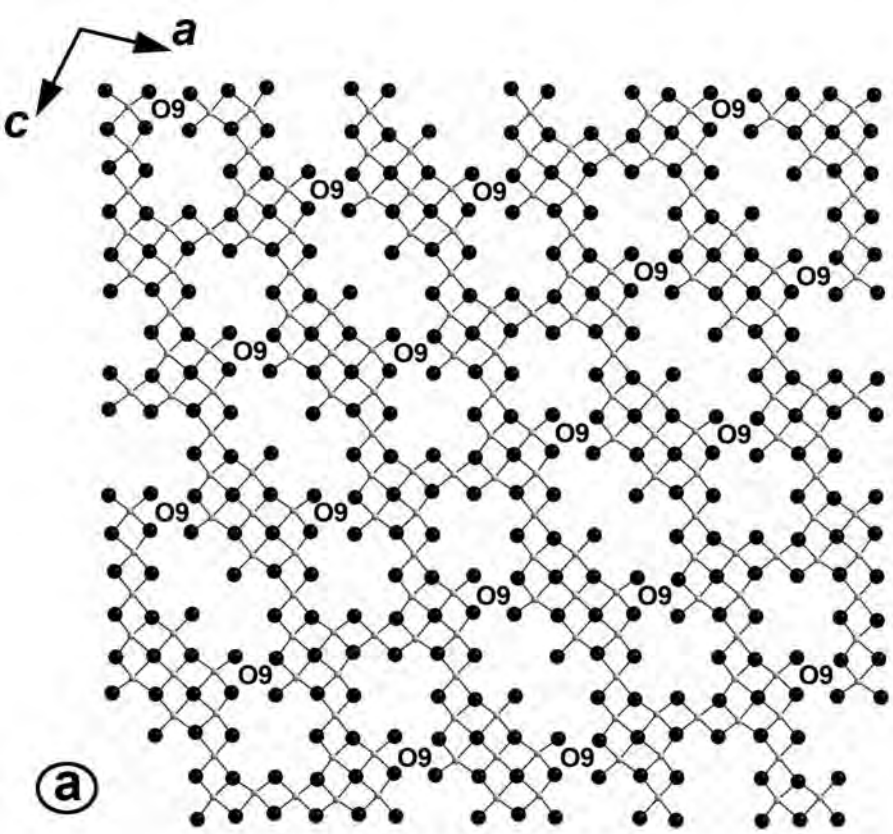
a
c
O9
a

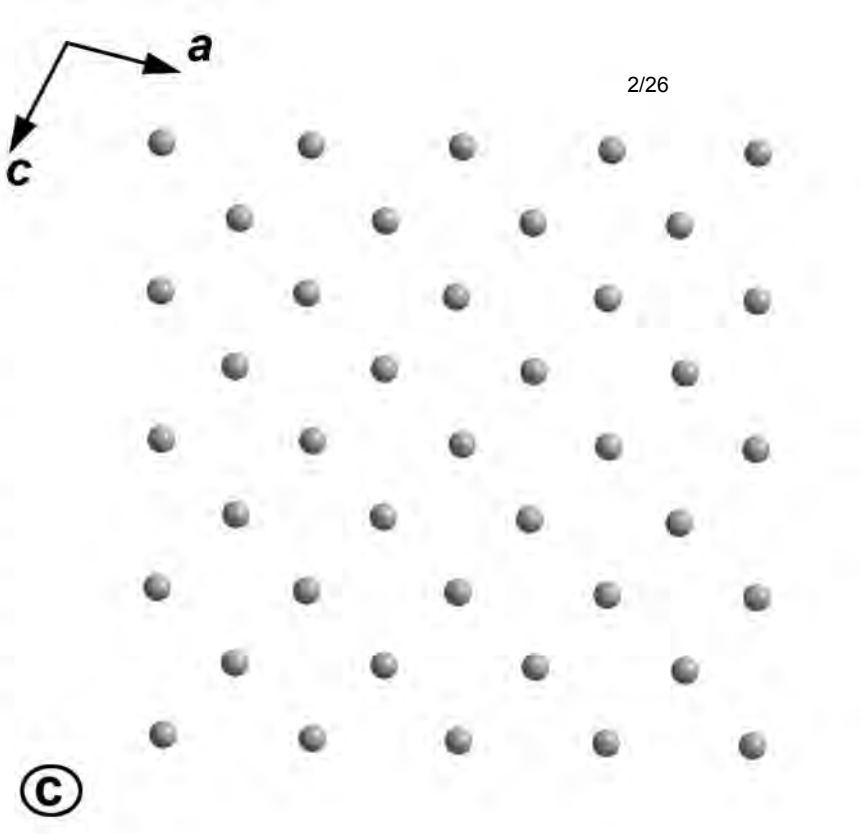
a
c
c

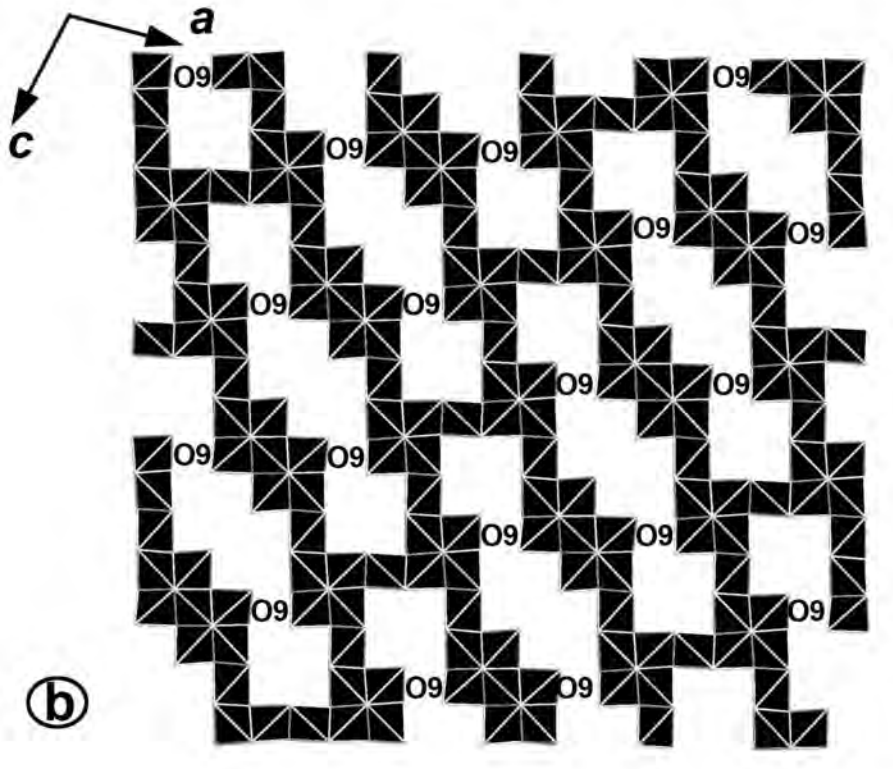
a
c
O9
b

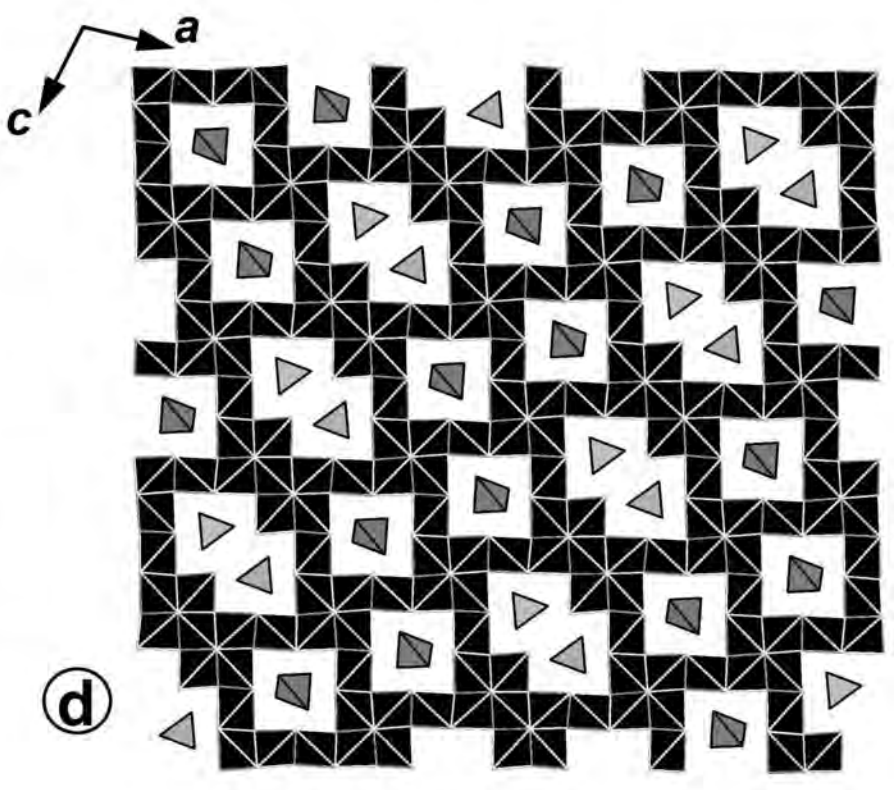
a
c
d

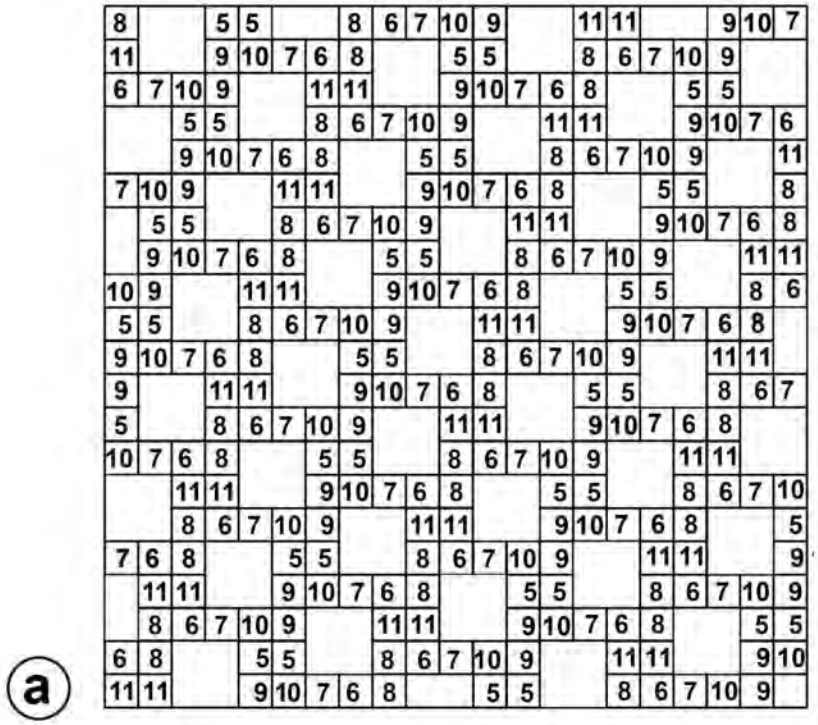

a

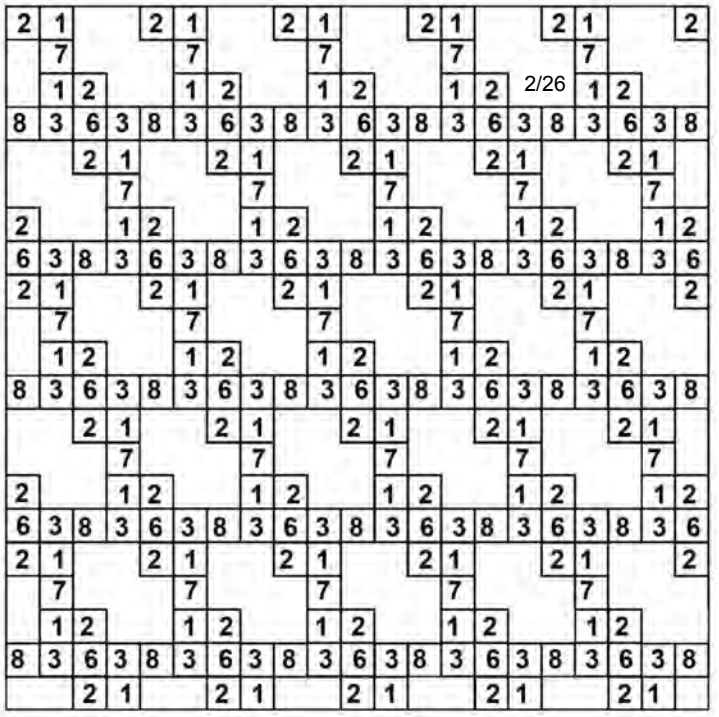

b

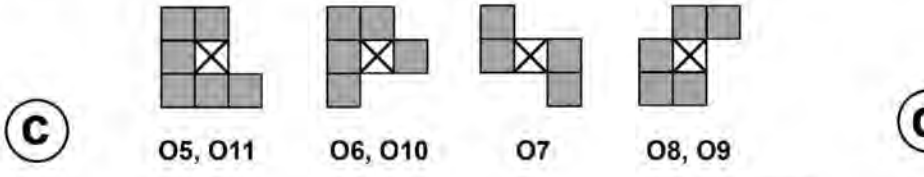

c

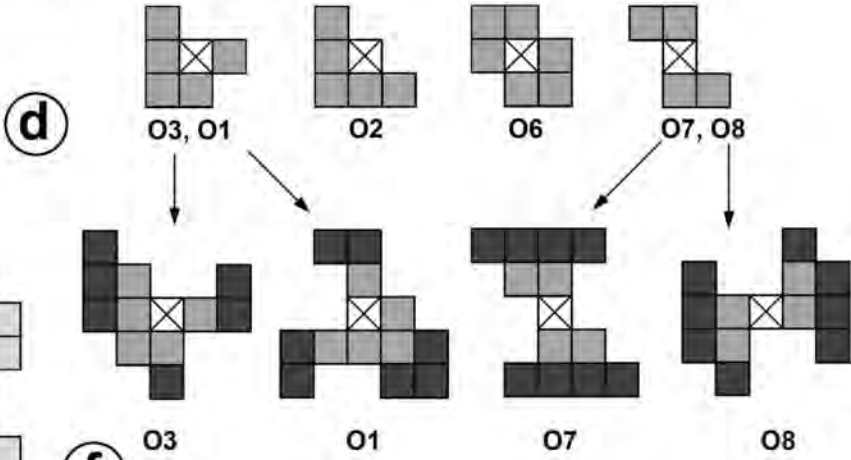

d

f

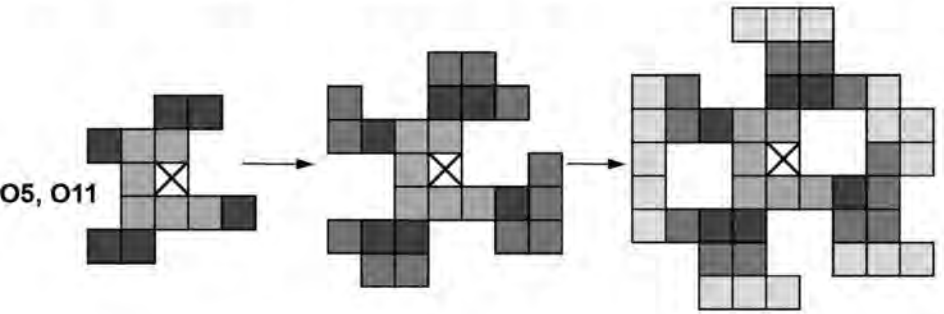

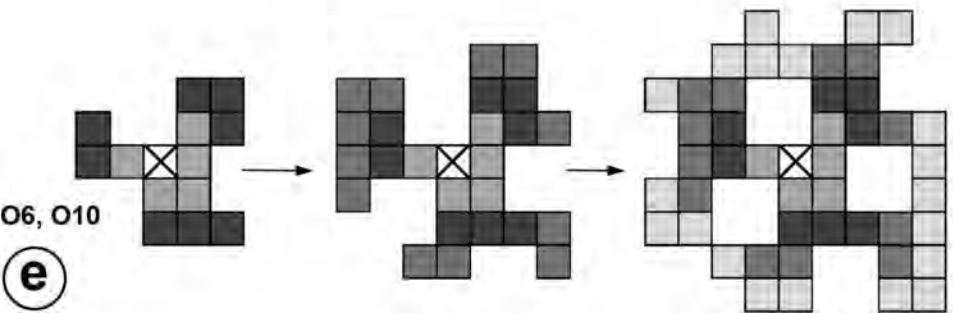

e

19	9	14	10			16			16			10	14	9	19	13	19	9	14
15			18			15	12			11	17	20	17	11			12	15	
16			10	14	9	19	13	19	9	14	10			16				16	
11	17	20	17	11			12	15			18			15	12			11	17	20
14	10			16				16			10	14	9	19	13	19	9	14	10	
	18			15	12			11	17	20	17	11			12	15			18	
	10	14	9	19	13	19	9	14	10			16				16			10	14
20	17	11			12	15			18			15	12			11	17	20	17	11
		16				16			10	14	9	19	13	19	9	14	10			16
		15	12			11	17	20	17	11			12	15			18			15
14	9	19	13	19	9	14	10			16				16			10	14	9	19
11			12	15			18			15	12			11	17	20	17	11		
16				16			10	14	9	19	13	19	9	14	10			16		
15	12			11	17	20	17	11			12	15			18			15	12	
19	13	19	9	14	10			16				16			10	14	9	19	13	19
	12	15			18			15	12			11	17	20	17	11			12	15
		16			10	14	9	19	13	19	9	14	10			16				16
		11	17	20	17	11			12	15			18			15	12			11
19	9	14	10			16			16			10	14	9	19	13	19	9	14	
15			18			15	12			11	17	20	17	11			12	15		
16			10	14	9	19	13	19	9	14	10			16				16		

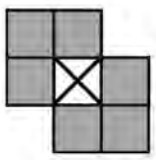

O13

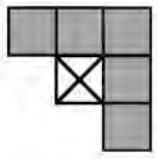

O12

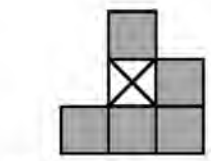

O10, O17, O11
O19, O14, O15

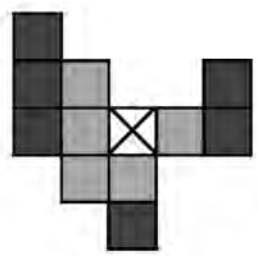

O19

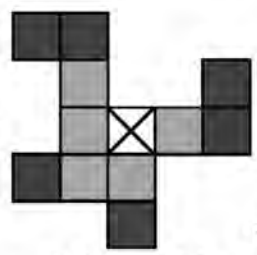

O17, O11,
O10, O14

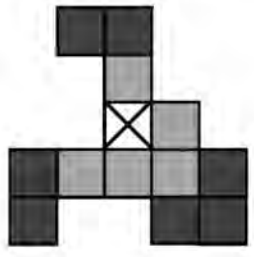

O15

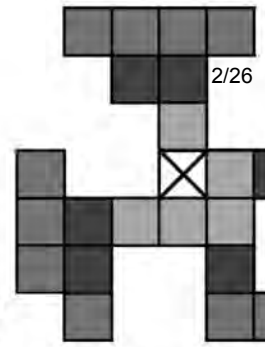

O11

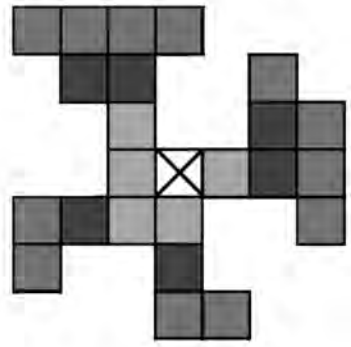

O17

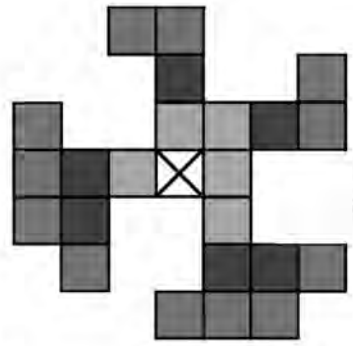

O14

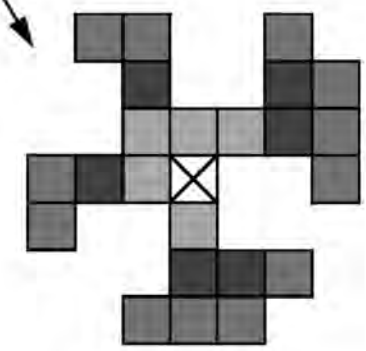

O10

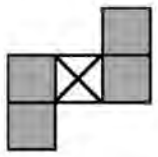

O9, O16,
O18, O20

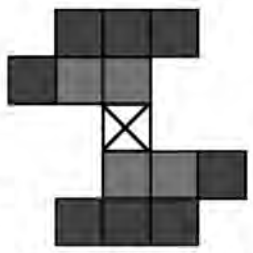

O9, O18, O20

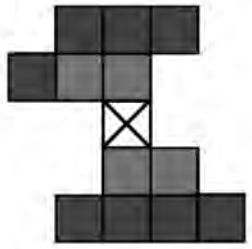

O16

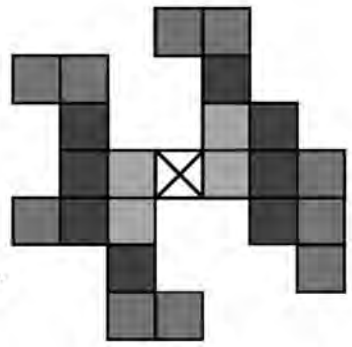

O9

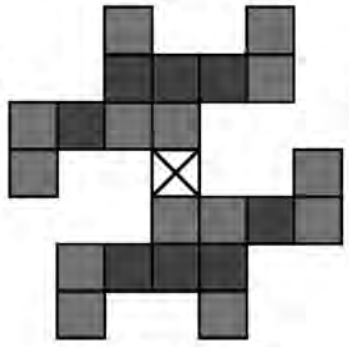

O18, O20

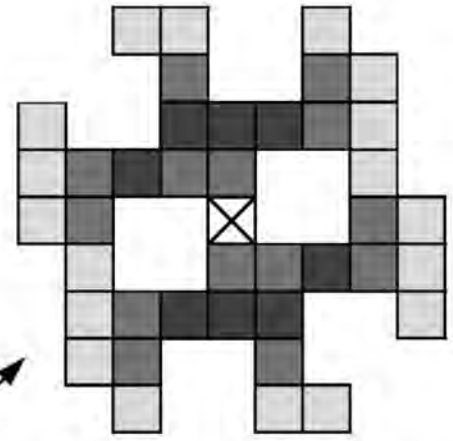

O18

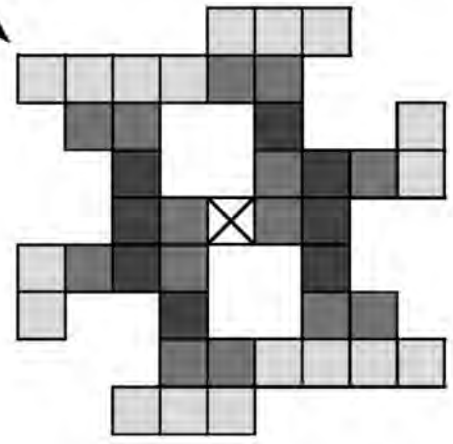

O20